

Submitted to *Biophysical Journal*  
January 16, 2006

**Lipid composition greatly affects the *in vitro* surface activity  
of lung surfactant protein mimics**

Shannon L. Seuryneck, Nathan J. Brown, Michelle T. Dohm,  
Cindy W. Wu, and Annelise E. Barron

*Department of Chemical and Biological Engineering, Northwestern University,  
2145 Sheridan Road, Evanston, Illinois 60208*

**Correspondence:**

Annelise E. Barron  
Associate Professor  
Northwestern University  
Department of Chemical and Biological Engineering  
2145 Sheridan Road  
Evanston, IL 60208  
(847) 491-2778 (t)  
(847) 491-3728 (f)  
a-barron@northwestern.edu

## Abstract

An important aspect of developing a functional, biomimetic lung surfactant (LS) replacement is the selection of the synthetic lipid and surfactant protein (SP) mimic components. Studies elucidating the roles of different lipids and surfactant proteins in natural LS have provided critical information necessary for the development of synthetic LS replacements that offer performance comparable to the natural material. In this study, the *in vitro* surface-active behaviors of peptide- and peptoid-based mimics of the lung surfactant proteins, SP-B and SP-C, were investigated using three different lipid formulations. The lipid mixtures were chosen from among those commonly used for the testing and characterization of SP mimics: (1) dipalmitoyl phosphatidylcholine : palmitoyloleoyl phosphatidylglycerol 7:3 [w/w] (**PCPG**), (2) dipalmitoyl phosphatidylcholine : palmitoyloleoyl phosphatidylglycerol : palmitic acid 68:22:9 [w/w] (**TL**), and (3) dipalmitoyl phosphatidylcholine : palmitoyloleoyl phosphatidylcholine : palmitoyloleoyl phosphatidylglycerol : palmitoyloleoyl phosphatidylethanolamine : palmitoyloleoyl phosphatidylserine : cholesterol, 16:10:3:1:3:2 [w/w] (**IL**). The lipid mixtures and lipid/peptide or lipid/peptoid formulations were characterized *in vitro* using a Langmuir-Wilhelmy surface balance, fluorescent microscopic imaging of surface film morphology, and a pulsating bubble surfactometer. Results show that the three lipid formulations exhibit significantly different surface-active behaviors, both in the presence and absence of SP-mimics, with desirable *in vitro* biomimetic behaviors being greatest for the TL formulation. Additionally, lipid composition greatly affects the extent of biomimicry in the surface-active behaviors of both peptoid- and peptide-based SP mimics.

## **Introduction**

Lung surfactant (LS) is a complex biomaterial that coats internal pulmonary surfaces and which is essential for normal breathing (Notter, 2000d; Poynter and LeVine, 2003). This surface-active material reduces and regulates surface tension within the alveoli during respiration (Lewis, 2003; Poynter and LeVine, 2003). The most important attributes of LS are that it is able to (i) adsorb rapidly to the air-water interface, (ii) reach near-zero surface tension upon film compression and prevent alveolar collapse, and (iii) respread at the air-water interface through multiple expansions and contractions of film surface area. The absence or dysfunction of lung surfactant results in neonatal respiratory distress syndrome (nRDS), a leading cause of infant mortality in the United States (Notter, 2000b). Currently, premature infants suffering from nRDS are treated by intratracheal instillation of an exogenous LS replacement, typically animal-derived, into the lung (Notter, 2000a). There are concerns associated with the use of animal-derived LS replacements, including high cost, batch-to-batch variability, and the potential for viral transmission (Frerking, 2001; Notter, 2000a). Less expensive, synthetic LS replacements have been developed, but are not commonly used due to the generally inferior efficacy they have so far shown for the treatment of nRDS (Notter, 2000a). This is attributed to the lack of the hydrophobic surfactant proteins (SPs) present in animal-derived surfactant that are necessary for the proper biophysical function of LS (Notter, 2000a; Robillard, 1964; Schram and Hall, 2004; Suresh and Soll, 2003). Hence, there is a need for an entirely synthetic LS replacement that contains good functional mimics of the hydrophobic surfactant proteins as well as the lipid portion of LS, and which is less expensive than animal-derived formulations.

In order to create a useful synthetic LS replacement, the role of each LS component must be considered carefully. Lipids comprise approximately 90% of LS, and proteins approximately

10% (Poynter and LeVine, 2003). The hydrophobic surfactant proteins, SP-B and SP-C, are thought to be responsible both for lipid organization and for the fluidity and respreadability of the lipid layer (Frerking, 2001; Goerke, 1997; Hall et al., 1992; Notter, 2000a; Wang et al., 1996; Notter, 2000c), and therefore are necessary for the proper biophysical functioning of LS. The addition of SP-B and/or SP-C to lipid mixtures generally results in a faster rate of adsorption, lower minimum surface tensions, and better respreadability of the film compared to the lipid mixture alone (Goerke, 1997; Hall et al., 1992; Notter, 2000c; Wang et al., 1996).

The major lipid class in LS is phosphatidylcholine (PC), comprising approximately 85% of LS lipids. Dipalmitoyl phosphatidylcholine (DPPC) is the most prevalent single component of LS, comprising nearly half of the PC species. Monolayers of DPPC are able to maintain near-zero surface tensions upon compression due to DPPC's ability to pack in an ordered fashion (Goerke, 1997; McLean and Lewis, 1995; Notter, 2000c). However, a stiff monolayer such as that formed by DPPC adsorbs relatively slowly to the air-aqueous interface and does not respread easily upon successive compressions and expansions of film area (Goerke, 1997; McLean and Lewis, 1995; Notter, 2000c). The addition of unsaturated phospholipids such as palmitoyloleoyl phosphatidylcholine (POPC) and palmitoyloleoyl phosphatidylglycerol (POPG) or other lipids and hydrophobic molecules such as palmitic acid (PA) and cholesterol has been shown to enhance the adsorption rate of the lipid film and to improve the respreadability of the monolayer; however the minimum surface tension upon compression is increased in comparison to DPPC films (Veldhuizen et al., 1998).

There is growing evidence that a functional replacement for natural LS must either contain SP-B and/or SP-C or comprise good functional mimics of these proteins. Both proteins have unique structural attributes which are not trivial to mimic with synthetic peptides or

peptidomimetics. SP-B is an amphipathic, predominantly helical protein that is 79 amino acids long (8.7 kDa in monomeric form) (Notter, 2000c), with 3 intramolecular disulfide bridges (Johansson et al., 1991) and one intermolecular disulfide bond, forming a homodimer (Beck et al., 2000; Noguee, 2004; Notter, 2000c; Wustneck et al., 2003). SP-B knockout mice die at birth (Clark et al., 1995), however, since SP-B is necessary for the processing of SP-C proprotein, these mice also lack functional SP-C (Vorbroker et al., 1995). SP-B directs LS surface activity through the control of lipid film organization (Krol et al., 2000; Notter, 2000c) and enhances monolayer adsorption and respreading (Gordon et al., 1996; Notter, 2000c). Other theories suggest that SP-B selectively removes non-DPPC lipids from the film upon compression, promoting monolayer enrichment in DPPC (Krol et al., 2000; Veldhuizen et al., 2000), sometimes referred to as the “squeeze-out” hypothesis. The disulfide bridge that connects the dimerized form of SP-B is thought to act as a hinge, effectively anchoring squeezed-out molecules to the monolayer (Takamoto et al., 2001).

While the chemical synthesis of an exact mimic of this 79mer protein is too difficult to be practical, studies of short segments of SP-B have shown that amphipathic, helical segments from both the *N*- and *C*-termini (SP-B<sub>1-25</sub> and SP-B<sub>53-78</sub>, respectively) are able to improve the biomimetic surface activity of lipid mixtures (Bruni et al., 1991; Lipp et al., 1997; Longo et al., 1993; Baatz et al., 1991). There is evidence, based on Langmuir trough studies, that the amino-terminal region, SP-B<sub>1-25</sub> is sufficient to retain much of the physiological function of synthetic SP-B<sub>1-78</sub> (Lipp et al., 1997; Longo et al., 1993). An analog of SP-B<sub>1-25</sub> with cysteine to alanine substitutions to prevent unwanted disulfide bond formation was shown to retain both the helical content and the essential surface activities of the human SP-B<sub>1-25</sub> sequence (Bruni et al., 1991).

SP-C is an amphipathic, helical protein, which is just 35 amino acids long (4.2 kDa) (Notter, 2000c). It is one of the most hydrophobic proteins known, due to its extremely high content of valine, leucine, and isoleucine (Notter, 2000c). The two cationic residues at positions 11 and 12 are thought to interact with anionic phospholipid head groups, promoting SP-C binding to the lipid layer (Creuwels et al., 1995). Cysteines at positions 5 and 6 are post-translationally palmitoylated, and these alkyl modifications are thought to be important for proper function; however, their exact function and the extent of their importance is a matter of debate (Bi et al., 2002; Flach et al., 1999; Gustafsson et al., 2000; Qanbar et al., 1996; Wang et al., 1996). The three-dimensional structure of human SP-C was solved by 2D-NMR in methanol (Johansson et al., 1994), and is dominated by an  $\alpha$ -helix 37 Å long. Within this helix is a 23 Å-long, valyl-rich stretch of hydrophobic amino acids. The length of the SP-C helix, and of the valyl-rich helical region, closely match the thickness of a DPPC bilayer and its acyl-chain portion (37 Å and 26 Å), respectively, suggesting that SP-C can traverse a phospholipid bilayer (Johansson et al., 1994). FTIR studies have shown that the SP-C helix orients in a transbilayer orientation in a fluid lipid film, so that the helical region interacts hydrophobically with lipid acyl chains (Gericke et al., 1997).

Due to SP-C's extreme hydrophobicity and strong tendency to aggregate and misfold in the absence of lipids, several different simplified peptide mimics of SP-C have been created and studied (Cochrane et al., 1996; Johansson et al., 1995; McLean et al., 1993; Takei et al., 1996a; Takei et al., 1996b). These peptides emulate SP-C's overall amphipathicity and its helical structure while moderating overall hydrophobicity and reducing the natural tendency for aggregation (Walther et al., 2000). Takei *et al.* synthesized various non-palmitoylated, full-length and truncated forms of SP-C with sequences otherwise identical to the natural protein, and

found that a core sequence (residues 5-31 or 6-32) was required for biophysical activity comparable to the full-length protein (Takei et al., 1996a). Nilsson *et al.* created an SP-C analog replacing valines with leucines and cysteines with serines, which showed surface activity comparable to native SP-C, but with a much-reduced tendency for hydrophobic aggregation and misfolding (into insoluble  $\beta$ -sheets) (Johansson, 2003; Nilsson et al., 1998). Takei *et al.* also showed that substitution of the entire poly-valyl region with leucine or norleucine residues in a truncated SP-C mimic results in a more tractable peptide that can mimic SP-C's surface activity both *in vitro* and *in vivo* (Takei et al., 1996b).

The biophysical functions of SP-B and SP-C overlap to some degree (Poynter and LeVine, 2003). Both full-length and *N*-terminal fragments of SP-C interact with lipid bilayers and promote lipid insertion to the air-liquid interface, enhancing the rate of surfactant film adsorption and respreading (Oosterlakendijksterhuis et al., 1991a; Plasencia et al., 2004; Qanbar et al., 1996; Taneva and Keough, 1994a; Wang et al., 1996). Dynamically, SP-C has been shown to lower the minimum surface tension of various lipid films and stabilize compressed surfactant films, but reportedly to a lesser extent than SP-B (Qanbar et al., 1996). A few studies have suggested that there is a lack of synergy between the biophysical functioning of SP-B and SP-C (Plasencia et al., 2001; Taneva and Keough, 1994b; Wang et al., 1996); certainly, further studies of this question are of interest. Since in some ways their biophysical activities are quite similar, it remains unknown why both SP-B and SP-C are so strictly conserved across species. However, it is clear that they each have important roles in LS function and should both be studied for use in a biomimetic LS replacement. Investigations of the specific molecular mechanisms by which SP-B and SP-C interact with lipids in monolayers, bilayers and multilayers are being actively pursued by biophysicists and physiologists (Alig et al., 2004;

Brockman et al., 2003; Cruz et al., 2004; Ding et al., 2003; Freitas et al., 2003; Haller et al., 2004; Harbottle et al., 2003; Krol et al., 2000; Markart et al., 2003; Morrow, 2004; Schram and Hall, 2004; Veldhuizen et al., 2000; Wustneck et al., 2001; Wustneck et al., 2003).

Sequence-specific poly-*N*-substituted glycines, or peptoids, are a particularly interesting class of peptidomimetics due to their facile and inexpensive solid-phase synthesis and the ease with which diverse side chains can be incorporated. Peptoids are generally synthesized using a submonomer approach developed by Zuckermann *et al.* (Zuckermann et al., 1992), and represent an alternate derivative of a polypeptide backbone, with the side chains attached to the amide nitrogens rather than to the  $\alpha$ -carbons (Simon et al., 1992; Zuckermann et al., 1992). The *N*-substituted backbone of this class of molecules resists proteolysis, resulting in enhanced bioavailability and the potential for reduced specific recognition by the immune system (Borman, 1998; Miller et al., 1995). *In vivo* and *in vitro* pharmacological characterization of selected peptoid trimers found them to be bioactive, non-toxic, and non-immunogenic (Gibbons et al., 1996). Such properties are of course extremely sequence- and size-dependent, and the biocompatibility of longer peptoid oligomers has not yet been assessed.

Although peptoids cannot form backbone-backbone hydrogen bonds like peptides to stabilize secondary structure, structural studies have shown that peptoid sequences with chiral side chains form stable helical structures with a chiral sense, similar to polyproline helices in peptides (Kirshenbaum et al., 1998). Peptoid helices have a helical pitch of approximately 6 Å and a periodicity of 3 residues per turn, and are stabilized primarily by steric and electronic repulsions (Armand et al., 1998). Detailed studies of peptoid sequence and chain length by CD and NMR led to some general rules for the formation of stable peptoid helices: (1) at least 50% of the side chains should be chiral and aromatic, (2) a chiral, aromatic side chain at the carboxy



terminus stabilizes the helix, (3) the helix is stabilized by an aromatic face, i.e., if aromatic side chains are positioned along one or more faces of the helix *via* 3-fold sequence patterning (Wu et al., 2001). Studies of a water-soluble 36mer peptoid revealed that the helical secondary structure is extremely robust, with no structural changes observed at both high temperatures and high urea concentrations (Sanborn et al., 2002), confirming that these helices are primarily stabilized by steric factors rather than by other more labile interactions such as hydrogen bonding, as had been previously hypothesized (Armand et al., 1997; Armand et al., 1998).

In previous studies we have investigated the surface-active behaviors of peptoid-based mimics of both SP-B and SP-C in lipid films and compared the activity of the peptoids to the respective peptide mimic (Seuryneck et al., 2005b; Wu et al., 2003). Both peptoid-based mimics were designed to capture the essential structural features of the cognate peptide: SP-B mimics were helical and facially amphipathic (Seuryneck et al., 2005b), while SP-C mimics were helical and longitudinally amphipathic (Wu et al., 2003). The surface-active behaviors of the peptoid mimics as well as of comparator peptides were characterized in biomimetic lipid films using a Langmuir-Wilhelmy surface balance and a pulsating bubble surfactometer, while film phase morphologies were observed using fluorescence microscopy in conjunction with a Langmuir trough. The peptoid mimics, which ranged from 17 to 22 monomers in length, were found to exhibit surface-active behaviors and film phase morphologies that were in many ways similar to, though not identical to the model peptide mimics (Seuryneck et al., 2005b; Wu et al., 2003).

The surface activities of various other SP mimics have been characterized in a multitude of different lipid formulations, including pure monolayers of DPPC (Bi et al., 2002; Cruz et al., 1997), DPPG (Bi et al., 2002; Lipp et al., 1997), and PA (Lipp et al., 1996). Because of the complexity of data interpretation for surfactant characterization techniques such as Infrared

Spectroscopy (IR) and X-ray scattering and diffraction, single-lipid films are often used for these types of investigations. For simpler techniques to investigate surface activity, formulations containing multiple lipid species have been used. Since both SP-B and SP-C are cationic and are thought to interact with anionic PG head groups (Baatz et al., 1990; Johansson et al., 1991; Oosterlakendijksterhuis et al., 1991b; Oosterlakendijksterhuis et al., 1992; Taneva and Keough, 1994a; Vandenbussche et al., 1992) and since DPPC is necessary for reaching low surface tensions, formulations composed of DPPC and POPG have often been used for the characterization of SPs and their mimics in lipid films with the pulsating bubble surfactometer, Langmuir-Wilhelmy surface balance, epifluorescence microscope, and Brewster angle microscope (Cruz et al., 2004; Dico et al., 1997a; Nag et al., 1996; Oosterlakendijksterhuis et al., 1991a; Yu and Possmayer, 1990; Yu and Possmayer, 1993; Dico et al., 1997b).

Tanaka *et al.* investigated 25 different surfactant formulations containing varying combinations of phospholipids (DPPC, PG, PS, PI, PE, and sphingomyelin), fatty acids (PA, palmitoleic acid, stearic acid, or oleic acid), acylglycerols, and a lipid-bound protein isolated from LS (Tanaka et al., 1986). Of these 25 formulations, they found three surfactant mixtures with good, apparently biomimetic, surface activities, all containing 68.0% DPPC, 22.1% PG or PS, 9.0% fatty acid (palmitic acid or stearic acid), and 0.9% protein [w/w]. Based on these results, a similar lipid formulation containing DPPC, POPG, and PA (68:22:9 [w/w], the so-called “Tanaka lipids” (TL)) has been used widely to investigate the surface activity of SP mimics both *in vitro* and in animal models of RDS (Amirkhanian et al., 1993; Amirkhanian et al., 1991b; Bringezu et al., 2001; Bringezu et al., 2002; Ding et al., 2001; Gupta et al., 2001; Gustafsson et al., 1996; Palmblad et al., 1999; Seuryneck et al., 2005b; Walther et al., 2002; Wu et al., 2003; Amirkhanian et al., 1991a; Waring et al., 1989).

While the Tanaka lipids have been shown to facilitate the biomimetic functioning of surfactant protein replacements both *in vivo* and *in vitro*, this simple formulation has a composition which differs greatly from that of natural surfactant lipids. Most notably, the DPPC content of the Tanaka lipids (69%) is significantly higher than that of natural LS and also of successful, commercially available LS replacements such as Infasurf™ (55%) (Walther et al., 2005). In addition, natural LS contains other anionic phospholipids that are likely to interact with the cationic amino acid side chains of SP-B and SP-C, such as phosphatidylinositol (PI), phosphatidylethanolamine (PE), and phosphatidylserine (PS), as well as cholesterol, which is believed to further fluidize the monolayer (Diemel et al., 2002; Discher et al., 2002; Fleming and Keough, 1988; Larsson et al., 2003; Malcharek et al., 2005; Notter et al., 1980; OGREIG and Daniels, 2001; Taneva and Keough, 1997; Tolle et al., 2002). Recent work by Walther *et al.* investigated the surface activity of three lipid formulations, including lipids isolated from lung lavage, a more complex formulation designed to be the synthetic equivalent of the natural LS lipids, and the Tanaka lipids, in combination with dimeric SP-B<sub>1-25</sub> both *in vitro* (captive bubble surfactometer) and *in vivo* (a rat washout model of RDS) (Walther et al., 2005). Studies performed on a captive bubble surfactometer indicate that the synthetic lung lavage lipid formulation that more closely mimics the composition of natural lung lavage lipids, containing DPPC, DOPC, POPG, POPE, POPS, and cholesterol (16:10:3:1:3:2 [w/w]), reached a minimum surface tension similar to that of both natural lipids and the Tanaka lipids. However, studies in a rat model of RDS revealed higher oxygenation levels with the natural lipids or the synthetic lung lavage lipids than with the Tanaka lipids. Therefore, this synthetic lipid formulation that more closely mimics the composition of natural LS seems to show greater promise for *in vivo* use as part of a biomimetic LS replacement.

In our previous studies, peptoid mimics of SP-B and SP-C in a Tanaka lipid film have been compared with their respective peptide analogs using the pulsating bubble surfactometer, Langmuir-Willhelmy surface balance, and fluorescence microscopic film imaging (Seurynck et al., 2005b; Wu et al., 2003). While, based on these *in vitro* studies, the peptoid-based SP mimics show promise for use in a biomimetic LS replacement, neither was able to entirely mimic the peptide/lipid interactions or the unique biophysical activities of natural LS. It has been shown that lipid formulation composition can play a large role in the surface activity and structure of a specific SP mimic (Walther et al., 2005). In this paper, we examine the *in vitro* function of two peptoid- and two peptide-based SP mimics in three different lipid formulations to further investigate specific SP mimic/lipid interactions. To our knowledge, this is the first time a comparative study such as this has been completed even for one SP-mimetic peptide; our study compares four different promising SP-mimics in three different interesting lipid formulations using a Langmuir-Willhelmy surface balance, a pulsating bubble surfactometer (with the determination of accurate data loops rather than just maximum and minimum surface tensions), and fluorescence microscopic imaging of surface film phase behavior. Our results show that these three lipid formulations exhibit significantly different surface-active behaviors, both in the presence and absence of SP-mimics. Additionally, we find that lipid composition has dramatic effects on the surface-active behaviors of both peptoid- and peptide-based SP mimics.

## **Materials and Methods**

### *Materials and reagents*

Peptide and peptoid synthesis reagents were purchased from Applied Biosystems (Foster City, CA) and Aldrich (Milwaukee, WI). Resins and Fmoc-protected amino acids were

purchased from NovaBiochem (San Diego, CA), while 2,2,5,7,8-pentamethylchroman-6-sulfonyl chloride (PMC) was purchased from Omega Chemical (Quebec, CA), and primary amines and di-*tert*-butyl dicarbonate (Boc) were purchased from Aldrich. Acetonitrile, isopropanol, and trifluoroacetic acid (TFA) were purchased from Fisher Scientific (Pittsburgh, PA). DPPC, POPG, POPC, POPE, POPS, and cholesterol were purchased from Avanti Polar Lipids (Alabaster, AL), PA was purchased from Aldrich, and Texas Red® 1,2-dihexadecanoyl-*sn*-glycero-3-phosphoethanolamine, triethylammonium salt (TR-DHPE) was purchased from Molecular Probes (Eugene, OR). All chemicals were used without further purification.

#### *Peptide and peptoid synthesis, purification, and characterization*

Cysteine-to-alanine substitutions were made at positions 8 and 11 in the peptide SP-B<sub>1-25</sub> to prevent unwanted disulfide bond formation (sequence shown in Table 1). We synthesized an SP-C-mimetic peptide with a sequence modified to prevent aggregation, SP-C<sub>F,F</sub>, that included valine-to-leucine and cysteine-to-phenylalanine substitutions (sequence shown in Table 1) (Davis et al., 1998; Nilsson et al., 1998). Both peptides were synthesized by standard Fmoc chemistry on solid support (pre-loaded Wang resin) using an ABI 433A automated peptide synthesizer (Applied Biosystems).

A peptoid-based mimic of SP-B, Peptoid B, was designed to mimic the helicity, facial amphipathicity, and hydrophobicity of SP-B<sub>1-25</sub>, as previously described (structure shown in Table 1) (Seurnyck et al., 2005b). A peptoid mimic of SP-C, Peptoid C, mimics residues 5-32 from human SP-C, with close sequence mimicry at the *N*-terminus and maintenance of the *C*-terminal hydrophobic helix (structure shown in Table 1) (Wu et al., 2003). Both peptoids were synthesized using an ABI 433A on Rink amide resin by the sub-monomer protocol previously described (Zuckermann et al., 1992). All molecules were cleaved from the resin with TFA,

along with the appropriate scavenging reagents, for 10 minutes or 1 hour depending on the sequence (the longer time is necessary to remove the PMC protecting group from guanidine side chains in SP-B<sub>1-25</sub>, SP-C<sub>F,F</sub>, and Peptoid C). SP-B mimics were purified by RP-HPLC using a linear gradient of 20%-95% solvent B in solvent A over 50 minutes (solvent A is 0.1% TFA in water [v/v] and solvent B is 0.1% TFA in acetonitrile [v/v]). SP-C mimics were purified by reversed-phase high performance liquid chromatography (RP-HPLC) using a linear gradient of 30%-80% solvent B in solvent A over 50 minutes (solvent A is 0.1% TFA in water [v/v] and solvent B is 0.1% TFA in acetonitrile-isopropanol 1:1 [v/v] for Peptoid C and 0.1% TFA in isopropanol [v/v] for SP-C<sub>F,F</sub>). The final purities of the molecules were confirmed to be > 97% by analytical RP-HPLC, and molecular weights were confirmed by electrospray mass spectrometry (SP-B<sub>1-25</sub> – 2866 Da, Peptoid B – 2592 Da, SP-C<sub>F,F</sub> – 3924 Da, Peptoid C – 3309 Da). The helicity of the peptides and peptoids was confirmed by circular dichroism spectroscopy (Seuryneck et al., 2005b; Wu et al., 2003).

#### *Sample preparation*

Each lipid was individually dissolved in chloroform/methanol (3/1 [v/v]) to a known concentration (~ 4 mg/mL). The lipids were combined to make three different formulations: PCPG lipids (DPPC:POPG, 7:3 [w/w]), Tanaka lipids (TL, DPPC:POPG:PA, 68:22:9 [w/w]), and synthetic Infasurf lipids (IL, DPPC:POPC:POPG:POPE:POPS:cholesterol, 16:10:3:1:3:2 [w/w]) with total lipid concentrations of ~ 2 mg/mL.

Peptide and peptoid mimics were dissolved in methanol to a known concentration (~ 2 mg/mL). The modified peptides, SP-B<sub>1-25</sub> and SP-C<sub>F,F</sub>, were added to the lipid mixtures at 10 weight percent, based on the total protein content in LS. The peptoid mimics were added to the lipids at the equivalent mole percentage (see Table 2).

### *Langmuir-Wilhelmy surface balance studies*

Surface pressure - molecular area isotherms were obtained using a home-built Langmuir-Wilhelmy surface balance, previously described (Seurnyck et al., 2005b). The trough was filled with 300 mL of aqueous buffer (150 mM NaCl, 5 mM CaCl<sub>2</sub>, 10 mM HEPES, pH 6.9) and heated to either 25 or 37 °C. The surfactant formulation was spread at the air-water interface from a chloroform/methanol solution using a glass syringe and allowed to equilibrate for 5 minutes. The barriers were then compressed and expanded at a rate of 30 mm/min. Surface pressure was measured using a Wilhelmy plate (Riegler and Kirsten GMBH, Berlin). Experiments were repeated for a total of six times per temperature for each surfactant formulation and were reproducible.

### *Fluorescence microscopic imaging*

In order to obtain fluorescence microscopic images, a Nikon MM40 compact microscope stand with a 100W mercury lamp (Tokyo, Japan) is used in conjunction with the Langmuir trough. Fluorescence is detected by a Dage-MTI three-chip color camera (Dage-MTI, Michigan City, IN) in conjunction with a generation II intensifier (Fryer, Huntley, IL). Samples were spiked with 0.5 mol% of a fluorescently labeled lipid, TR-DHPE, for detection. Previous studies have shown that inclusion of the labeled lipid at this concentration does not alter surfactant film morphology (Bringezu et al., 2001). Experiments were performed on an aqueous buffered subphase at 25 or 37 °C with a barrier speed of 5 mm/min, and were repeated for a total of three times per temperature for each surfactant formulation and were reproducible.

### *Pulsating bubble surfactometry*

A modified pulsating bubble surfactometer (General Transco, Largo, FL), previously described (Seurnyck et al., 2005a), was used to obtain both static-bubble and dynamic-bubble

adsorption data. An image acquisition system has been added to a commercial PBS in order to track bubble shape and size in real time. Images and pressure data from the instrument are sent to a LabVIEW program that is used to fit the bubble to an ellipse and calculate both the surface tension and the surface area of the bubble (Seuryneck et al., 2005a). Some of the major differences observed with the image analysis system are higher maximum surface tensions, reduced hysteresis in the data loop, and a reduced slope upon expansion of the bubble compared to the commercial PBS. These differences have been shown to reflect a more accurate measurement and representation of the surface-active behaviors of a biomimetic LS formulation (Seuryneck et al., 2005a).

Surfactant formulations were dried from the chloroform/methanol solution using a DNA 120 speedvac (Thermo Electron, Holbrook, NY), forming a pellet. The pellet was suspended in an aqueous buffer (150 mM NaCl, 5 mM CaCl<sub>2</sub>, 10 mM HEPES, pH 6.9) to 1.0 mg lipid/mL, with a final volume of 70-80  $\mu$ L. The surfactant formulations were mixed with a micropipette, sonicated with a Fisher Model 60 probe sonicator, and then mixed with a micropipette again to form a uniform solution. Samples were loaded into a sample chamber (General Transco) with putty placed on the capillary end of the sample chamber; the putty was removed before experiments were performed. A similar method has previously been shown to prevent sample leakage into the capillary (Putz et al., 1994).

All experiments were performed at physiological temperature, 37 °C. Static adsorption surface tension data were collected for 20 minutes or until equilibrium surface tension was reached, starting with a bubble radius of 0.4 mm and allowing the bubble size to drift (grow) throughout the adsorption period. Dynamic adsorption data were obtained at a frequency of 20 cycles/min until the shape of the hysteresis loop remained unchanged for at least 2 minutes



following static adsorption, again starting with a minimum bubble radius of 0.4 mm and allowing the bubble size to drift (grow) throughout the experiment. PBS experiments were repeated for a total of six times for each surfactant formulation and were reproducible.

## **Results and Discussion**

### *Comparison of lipid formulations*

The surface-active behavior of SP mimics can vary greatly in different lipid formulations. Here we have investigated the surface activities of four SP mimics in three different lipid formulations: “**PCPG**”, composed of DPPC and POPG (7:3 [w/w]); “Tanaka lipids (**TL**)”, composed of DPPC, POPG, and PA (68:22:9 [w/w]); and “synthetic Infasurf lipids (**IL**)”, based on the composition of the lipid portion of natural LS (Walther et al., 2005) and composed of DPPC, POPC, POPG, POPE, POPS, and cholesterol (16:10:3:1:3:2 [w/w]). The *in vitro* surface activities of the three lipid formulations were investigated using a Langmuir-Wilhelmy surface balance (LWSB), fluorescence microscopic (FM) imaging, and a pulsating bubble surfactometer (PBS).

An LWSB is typically used to record surface pressure ( $\Pi$ ) - molecular area ( $A$ ) isotherms. Lipids are spread at the air-aqueous interface in the 2D gaseous phase, at a high enough molecular area so that the lipid tails do not interact with one another and the surface pressure is essentially independent of molecular area. As the barriers are compressed, lipid tails begin to interact, entering the liquid expanded (LE) phase, and an increase in surface pressure is observed (referred to as lift-off). For natural LS, lift-off is expected to occur at a high molecular surface area ( $> 100 \text{ \AA}^2/\text{molecule}$ ) (Alonso et al., 2004). As the barriers are further compressed a coexistence of LE and liquid condensed (LC) phases is observed. A biomimetic plateau in the

isotherm between 40 and 50 mN/m, which is thought to correspond to a 2D phase transition and/or to the removal of non-DPPC components from the monolayer (Alonso et al., 2004), is typically observed for effective LS formulations. Finally, at high surface pressures the solid phase is observed, and for LS formulations we expect to see a collapse pressure near 70 mN/m corresponding to a surface tension of 0 mN/m (Alonso et al., 2004).

$\Pi$ -A isotherms taken at 25 °C for the three lipid formulations with no mimic added (**Figure 1A**) reveal that TL exhibit a much later lift-off ( $\sim 95 \text{ \AA}^2/\text{molecule}$ ) than either PCPG or IL ( $\sim 110 \text{ \AA}^2/\text{molecule}$ ). This trend is also observed, though less dramatically, at 37 °C (**Figure 1B**), with a lift-off area of  $\sim 100 \text{ \AA}^2/\text{molecule}$  for TL,  $\sim 110 \text{ \AA}^2/\text{molecule}$  for PCPG, and  $\sim 120$  for IL. All  $\Pi$ -A isotherms have at least a small kink at  $\sim 55 \text{ mN/m}$  at 25 °C with more pronounced plateaus for TL and IL, and at 37 °C all lipid formulations have small plateaus at  $\sim 50 \text{ mN/m}$ . Finally, with the exception of IL at 37 °C, collapse pressures are all near 70 mN/m. Interestingly, at 37 °C IL exhibits a low collapse pressure, of approximately 55 mN/m. While IL films were previously studied, LWSB results were not reported by Walther *et al.* (Walther et al., 2005).

The later lift-off area observed with the TL film in comparison to those of PCPG and IL is likely due to the inclusion of PA in only the TL formulation. Because PA is a single-chain lipid it occupies less space in the monolayer and therefore it takes a greater degree of film compression for the lipid tails to begin interacting with one another. Furthermore, IL contains more unsaturated lipids, which have kinked tails that take up more space in the monolayer, than either PCPG or TL ( $\sim 49\%$  for IL versus  $\sim 30\%$  for PCPG and  $\sim 22\%$  for TL). This leads to lift-off at a higher molecular area for IL films. Most likely, the inclusion of cholesterol in the IL formulation leads to more disorder at higher surface pressures, especially at higher temperatures

such as 37 °C (Notter, 2000e). This provides an explanation for why the lipid film is not able to reach high surface pressures, nor to make the transition from the LC phase to a solid phase without film collapse.

The surface phase morphologies of the lipid films were observed using FM imaging in conjunction with the LWSB. FM images were obtained by spiking the samples prepared for LWSB studies with 0.5 mol% TR-DHPE. The bulky fluorescent tag tends to reside predominantly in the LE phase, which appears as the bright regions in the images, while the LC phase tends to exclude the fluorescently labeled lipid and appears relatively dark. In **Figure 2**, FM images are shown for PCPG (A-B), TL (C-D), and IL (E-F) films at 37 °C, from a point on the isotherm just before the plateau, ~ 35 mN/m (left panels: A, C, E), and during the plateau, ~ 50 mN/m (right panels: B, D, F). At ~ 35 mN/m, no distinct LC domains are observed for either PCPG or IL, while dark LC domains are seen in the TL film. At ~ 50 mN/m, vesicle formation is observed for all of the lipid formulations (as evidenced by bright domains). However, the fundamental phase morphologies at ~ 50 mN/m are very different for the three formulations. In the case of both the PCPG and IL films, the vesicles are large and are likely forming below the monolayer (Gopal and Lee, 2001), confirming the squeeze-out theory that states that material is removed from the monolayer during the plateau (Krol et al., 2000; Takamoto et al., 2001; Veldhuizen et al., 2000). The TL film still exhibits LC domains of about the same size as those observed at ~ 35 mN/m, but with several small vesicles (bright spots) interspersed throughout.

Static-bubble PBS experiments were performed to observe the adsorption of the surfactant formulations to the air-liquid interface. Natural LS is expected to show a rapid decrease in surface tension to near 25 mN/m within less than one minute of initial adsorption (Scarpelli et al., 1992; Seuryneck et al., 2005a). Not unexpectedly, the lipid formulations with no

added SP mimics do not adsorb rapidly to the interface, nor do they reach low equilibrium surface tensions (**Figure 3A**). After 20 minutes of adsorption, PCPG reaches an equilibrium surface tension of  $\sim 55$  mN/m, TL  $\sim 50$  mN/m, and IL  $\sim 55$  mN/m. The lower surface tension reached by the TL film versus the PCPG film is likely due to a higher fluidity of the TL film caused by the presence of PA, which occupies a smaller molecular area in the monolayer. The high surface tension obtained with the IL film is likely due to the highly ordered phases that cholesterol induces at low surface pressures, which can preclude lipid adsorption to the interface in certain regions (Notter, 2000e).

Surface tension ( $\gamma$ ) vs. surface area ( $A$ ) data loops may be collected by running the PBS in the dynamic-bubble mode, with a cycling rate similar to that for adult respiration (20 cycles/min). The  $\gamma$ - $A$  loop for natural LS containing SPs is expected to exhibit a maximum surface tension ( $\gamma_{\max}$ ) of about 30 mN/m and a minimum surface tension ( $\gamma_{\min}$ ) near zero, with near-zero surface tension reached after a small amount of compression (reflected by a large extent of hysteresis in the data loop) (Scarpelli et al., 1992; Seuryneck et al., 2005a). The  $\gamma$ - $A$  loops obtained using the modified PBS for PCPG, TL, and IL are shown in **Figure 3B**. As expected, both  $\gamma_{\max}$  and  $\gamma_{\min}$  for all formulations are significantly higher than what is typically observed for natural LS ( $\gamma_{\max} \sim 65$  mN/m and  $\gamma_{\min} \sim 20$  mN/m for lipid formulations), and do not differ greatly from one another. In addition, we observe essentially no hysteresis in any of the data loops. In the case of the TL film, the slope upon expansion is quite high, meaning the elasticity of the film is high. This is not the case for either the PCPG or IL films, meaning that they have lower film elasticities (Ingenito et al., 1999).

### *In vitro surface-active behaviors of peptide and peptoid mimics in various lipid formulations*

In order to investigate the interactions of peptoids and model peptides with different types of lipids, experiments were performed with SP-B<sub>1-25</sub>, Peptoid B, SP-C<sub>F,F</sub>, or Peptoid C (**Table 1**) added to each of the lipid formulations. SP-B<sub>1-25</sub> and SP-C<sub>F,F</sub> were added to each lipid formulation at 10 weight percent (wt %), based on work by other researchers [REFs], while Peptoid B and Peptoid C were added to the lipids at the mole percentage equivalent to 10 weight percent of the respective peptide (see Table 2). Surface activities were investigated using the LWSB, FM imaging, and the PBS. As it has been discussed, many features of LWSB and PBS data have been correlated with the unique behavior and physiological functions of natural LS, but it is not conclusively known which of these properties are most important for biomedical efficacy. However, it can be assumed that a formulation that closely emulates the *in vitro* surface-active behaviors of natural LS is most likely to provide *in vivo* activity which is similar to that of natural LS.

$\Pi$ -A isotherms obtained at 37 °C reveal that when any of the mimics is added to any one of the lipid formulations, the lift-off area is substantially increased and the resulting plateau (when applicable) is more pronounced (**Figure 4**). Similar results are observed at 25 °C (data not shown). For the PCPG film, the addition of the SP-B<sub>1-25</sub> peptide increased the lift-off area to  $\sim 130 \text{ \AA}^2/\text{molecule}$ , while the addition of Peptoid B increased the lift-off area to  $\sim 115 \text{ \AA}^2/\text{molecule}$  (**Figure 4A**). The addition of Peptoid B to the PCPG film results in a much more pronounced plateau between 45 and 50 mN/m. With the addition of either of the two SP-C mimics, we observe only a slight increase in lift-off area, to  $\sim 117 - 120 \text{ \AA}^2/\text{molecule}$  (**Figure 4B**). However, the addition of the SP-C<sub>F,F</sub> peptide to PCPG results in a low film collapse pressure of  $\sim 50 \text{ mN/m}$ , indicating that the film is not able to form a stable solid phase. The film

containing SP-B<sub>1-25</sub> exhibits a higher lift-off area than the other SP mimic-containing films, however both Peptoid B and SP-C<sub>F,F</sub> provide much more pronounced biomimetic plateaus.

In the TL film, SP-B<sub>1-25</sub> exhibits a lift-off area of  $\sim 120 \text{ \AA}^2/\text{molecule}$ , while Peptoid B exhibits a lift-off area of  $\sim 110 \text{ \AA}^2/\text{molecule}$ , SP-C<sub>F,F</sub> exhibits a lift-off area of  $\sim 120 \text{ \AA}^2/\text{molecule}$ , and Peptoid C exhibits a lift-off area of  $\sim 115 \text{ \AA}^2/\text{molecule}$  compared to  $\sim 100 \text{ \AA}^2/\text{molecule}$  for the TL film without any additives (**Figures 4C and 4D**). In all instances the collapse pressure is high ( $\sim 70 \text{ mN/m}$ ) and a kink or plateau is observed between 45 and 50 mN/m, with more pronounced plateaus for the films with added SP-B<sub>1-25</sub>, Peptoid B, or SP-C<sub>F,F</sub>. Amongst the TL films, those containing either SP-B<sub>1-25</sub> or SP-C<sub>F,F</sub> exhibit earlier lift-off areas and more pronounced plateaus than the films containing the peptoid-based mimics.

The lift-off area for the IL film is increased with the addition of all SP mimics (to  $\sim 145 \text{ \AA}^2/\text{molecule}$  for SP-B<sub>1-25</sub> and Peptoid B,  $\sim 135 \text{ \AA}^2/\text{molecule}$  for SP-C<sub>F,F</sub>, and  $\sim 130 \text{ \AA}^2/\text{molecule}$  for Peptoid C (Figures 4E and 4F)). These lift-off areas are significantly higher than those observed for either the PCPG or TL films, probably due to the higher concentrations of unsaturated lipids with bulky tails. However, the collapse pressure for all of the IL films is significantly lower ( $\sim 50 \text{ mN/m}$ ) indicating that it is not able to form a stable condensed film. As previously mentioned, this early collapse is likely due to the tendency of cholesterol to create disordered phases at higher surface pressures (Notter, 2000e). In the IL films, SP-B<sub>1-25</sub> exhibits an earlier lift-off area than the other mimics, and all of the films exhibit extended plateau regions.

In **Figure 5**, FM images are shown for PCPG alone (A and B) and with added SP-B<sub>1-25</sub> (C and D), Peptoid B (E and F), SP-C<sub>F,F</sub> (G and H), or Peptoid C (I and J) at 37 °C from before the plateau,  $\sim 35 \text{ mN/m}$  (A, C, E, G, I), and during the plateau,  $\sim 50 \text{ mN/m}$  (B, D, F, H, J). FM

images for TL and IL films without and with added mimics are shown in **Figures 6** and **7** respectively (panels labeled as described above). At  $\sim 35$  mN/m, no domain formation is observed for any of the PCPG or IL formulations, while dark LC domains are observed for all of the TL formulations. Both the size and spacing of the domains are similar for all of the films except that containing Peptoid C, which shows significantly smaller LC domains and a slightly tighter packing density.

At  $\sim 50$  mN/m, domain formation is observed for all of the films. Bright domains, indicative of vesicle formation, are observed for all of the PCPG films (Figure 5). The addition of SP-B<sub>1-25</sub> or Peptoid B to PCPG results in the formation of large, bright circular domains, with SP-B<sub>1-25</sub> having very large domains. These types of domains are indicative of vesicle formation below the monolayer (Gopal and Lee, 2001). The addition of SP-C<sub>F,F</sub> or Peptoid C, however, results in the formation of large quantities of small bright vesicles, which appear to reside predominantly within the monolayer. At  $\sim 50$  mN/m dark LC domains are still observed for the TL films (**Figure 6**). However, for those films containing SP mimics, scattered small, bright vesicles are also observed. The SP-B<sub>1-25</sub>-containing film has very few vesicles, while the films containing Peptoid B and Peptoid C exhibit significantly more and SP-C<sub>F,F</sub> shows an even larger number, making it difficult to observe the dark LC domains. Like the PCPG films, the IL films only exhibit bright vesicle domains at  $\sim 50$  mN/m (**Figure 7**). The IL film containing SP-B<sub>1-25</sub> exhibits very large, bright domains, while that containing Peptoid B has medium-sized bright domains interspersed with small bright vesicles. Finally, the SP-C mimic-containing films show a large number of small bright vesicles.

Static-bubble adsorption data from the PBS reveal a substantial increase in the surfactant adsorption rate with the addition of mimics to any of the lipid formulations (**Figure 8**). In a

PCPG film (panels A and B), SP-B<sub>1-25</sub> facilitates a low equilibrium surface tension of  $\sim 20$  mN/m after approximately 7 minutes, while the film containing Peptoid B only reaches an equilibrium surface tension of  $\sim 30$  mN/m after approximately 15 minutes, indicating more rapid adsorption to the interface for SP-B<sub>1-25</sub> films than Peptoid B films. Rapid adsorption to the interface is observed for SP-C<sub>F,F</sub> films, with an equilibrium surface tension of  $\sim 25$  mN/m reached in less than one minute. Peptoid C films also reach an equilibrium surface tension of  $\sim 25$  mN/m, but require nearly 10 minutes for complete adsorption. In TL (panels C and D), films containing either SP-C<sub>F,F</sub> or Peptoid C reach a low equilibrium surface tension of  $\sim 25$  mN/m after only about 2 minutes. Peptoid B films also reach an equilibrium surface tension of  $\sim 25$  mN/m, but require nearly 5 minutes to adsorb. Films containing SP-B<sub>1-25</sub> only reach a surface tension of  $\sim 30$  mN/m after about 7 minutes.

In the TL films it again appears that SP-C mimics are able to facilitate much more rapid adsorption to the interface than SP-B mimics. In IL (panels E and F), films containing SP-C<sub>F,F</sub> and Peptoid C again reached a low equilibrium surface tension of  $\sim 25$  mN/m, with an adsorption time of less than a minute for SP-C<sub>F,F</sub> and about 2 minutes for Peptoid C. SP-B<sub>1-25</sub> and Peptoid B films also reach an equilibrium surface tension of  $\sim 25$  mN/m, but take much more time to adsorb ( $\sim 7$  minutes for SP-B<sub>1-25</sub> and  $\sim 13$  minutes for Peptoid B). In all lipid formulations, the SP-C mimics are able to facilitate more rapid adsorption to low equilibrium surface tensions than the SP-B mimics.

Dynamic-bubble PBS experiments reveal a substantial increase in biomimetic surfactant activity with added SP mimics (**Figure 9**). For all SP mimic-containing films, a decrease in  $\gamma_{\max}$  and an increase in hysteresis are observed. However, the maximum surface tensions reached by films containing peptide-based mimics are significantly lower than for films containing peptoid-



based mimics. In PCPG films (**Figures 9A** and **9B**) only the addition of SP-B<sub>1-25</sub> facilitates a decrease in  $\gamma_{\min}$ , from  $\sim 20$  mN/m to  $\sim 10$  mN/m, with a slight increase in hysteresis at high surface areas also observed. An increase in hysteresis at low surface areas is observed for films containing Peptoid B or SP-C<sub>F,F</sub>. Interestingly, Peptoid C-containing films show only a slight decrease in  $\gamma_{\max}$  and a very small increase in hysteresis at low surface tensions, otherwise the shape of the data loop is very similar to the PCPG film containing no additives. This indicates that Peptoid C is not significantly enhancing the dynamic surface activity of this lipid film, which is surprising considering the experimental findings obtained with the LWSB and FM, as well as the static PBS results.

In TL films (**Figures 9C** and **9D**)  $\gamma_{\max}$  is reduced to  $\sim 45$  mN/m with added SP-B<sub>1-25</sub>,  $\gamma_{\max} \sim 50$  mN/m with added Peptoid B,  $\gamma_{\max} \sim 32$  mN/m with added SP-C<sub>F,F</sub>, and  $\gamma_{\max} \sim 40$  mN/m with added Peptoid C, as compared to  $\sim 65$  mN/m for the lipid film. Interestingly, the SP-C mimics are clearly able to reduce  $\gamma_{\max}$  more sufficiently than the SP-B mimics. The  $\gamma_{\min}$  is decreased to near zero for all SP mimic-containing films. Since bubble shape greatly deforms from that of an ellipse at near-zero surface tensions, the image analysis system is not able to track bubble shape and therefore is not able to calculate the surface area or surface tension of the bubble. However, it is clear that near-zero surface tensions are obtained in these instances because the pressure drop is very low and the bubble shapes were highly deformed. Note however that these low-surface tension data points are not shown on the plots; these data had to be omitted from the dynamic PBS plots for both TL/Peptoid B films (**Figure 9C**) and TL/SP-C<sub>F,F</sub> and TL/Peptoid C films (**Figure 9D**). While a slight increase in data hysteresis is observed for films containing SP-B<sub>1-25</sub>, SP-C<sub>F,F</sub>, and Peptoid C, a large amount of hysteresis is observed for Peptoid B films, similar to what is expected for natural LS.

In IL (**Figures 9E and 9F**)  $\gamma_{\max}$  is decreased and hysteresis is increased with added SP mimics, while  $\gamma_{\min}$  remains the same as the lipid film at  $\sim 20$  mN/m. Similar to the PCPG films,  $\gamma_{\max}$  is decreased to a greater extent with added peptide mimics ( $\sim 45$  mN/m) than peptoid mimics ( $\sim 60$  mN/m). Films containing Peptoid B, SP-C<sub>F,F</sub>, or Peptoid C all show increased hysteresis at both high and low surface areas, while SP-B<sub>1-25</sub> films only have increased hysteresis at high surface areas.

Based on the dynamic-bubble PBS results, it appears that only TL formulations with added SP mimic are able to reach near-zero minimum surface tensions upon film compression. However, IL formulations with added SP mimics reach their minimum surface tension with less compression than TL formulations. The main difference between these lipid formulations is that TL contains PA while IL does not, and that IL contains cholesterol while TL does not. To greater elucidate the role and importance of these two different surfactant components, we designed five lipid formulations that either excluded cholesterol from IL or added PA to the IL formulation. No significant differences in the minimum surface tensions nor the extent of hysteresis in the PBS data loops were observed for these variant IL lipid formulations in combination with Peptoid B (data not shown). Hence, these compositional differences do not appear to be exclusively responsible for the unusual behavior of IL-based films.

## Conclusions

Previous work has shown that the addition of either Peptoid B or Peptoid C to TL improves the surface-active behavior of the LS replacement relative to what is observed for the lipids alone, and that both peptoid mimics show surface activities similar to or better than that of their respective peptide analogues (Seurnyck et al., 2005b; Wu et al., 2003). Although surfactant

film properties compared well with those exhibited by the TL/peptide formulations, they were unable to achieve the performance exhibited by natural LS (Scarpelli et al., 1992; Seuryneck et al., 2005a). In particular, dynamic-bubble PBS experiments revealed that the TL/Peptoid B formulation was able to reach near-zero  $\gamma_{\min}$ , but that  $\gamma_{\max}$  was significantly higher than the 35 mN/m expected for natural LS (Seuryneck et al., 2005b). In order to create a fully functional, synthetic LS replacement, the optimal lipid formulation must be further investigated.

In this paper we have investigated the *in vitro* behavior of peptide- and peptoid-based SP mimics in combination with three lipid formulations: PCPG, TL, and IL. These lipid formulations are composed of different types of lipids, allowing the investigation of specific SP mimic/lipid interactions. These studies have shown that lipid composition significantly affects the *in vitro* surface activities of the SP mimics. Specifically, combination of SP mimics with PCPG or IL results in a significantly higher lift-off. However, these more fluid films are not always able to reach the desired high collapse pressures. While TL films form LC domains at both  $\sim 35$  mN/m and  $\sim 50$  mN/m, FM imaging of PCPG or IL films reveals no domain formation at  $\sim 35$  mN/m and only vesicle formation at  $\sim 50$  mN/m. Finally, dynamic bubble PBS results show that SP mimics in PCPG or IL films are not able to reach near-zero minimum surface tensions, while SP mimics in TL films are. However, IL films especially are able to reach a minimum surface tension after a small amount of compression. Further investigation of lipid formulations containing varying amounts of cholesterol or PA in the IL film revealed little effect on the amount of hysteresis and the minimum surface tension.

None of these SP mimic/lipid formulations are able to precisely emulate the surface-active behavior of natural LS, however the TL formulation appears to come closest based on these *in vitro* studies. While a more complex lipid formulation based on the lipid composition of

Infasurf™ showed some promising results, even with added SP mimics the collapse surface pressure as observed by LWSB is quite low (~ 50 mN/m) and the minimum surface tension as observed by dynamic-bubble PBS experiments is quite high (~ 20 mN/m). Further experiments will be performed using *in vivo* models of RDS to study the efficacy of these formulations, and to shed further light on the relationship between these types of *in vitro* observations of surfactant behavior and the physiological functioning of surfactant replacements for the treatment of respiratory distress syndrome.

### **Acknowledgements**

We thank Dr. Mark Johnson and Dr. Ronald N. Zuckermann for their assistance. This work was supported by the National Science Foundation (Grant Nos. BES-9870386 and BES-0101195) and the National Institutes of Health (Grant No. 1R01HL67984-01).

## References

- Alig, T.F., H.E. Warriner, L. Lee, and J.A. Zasadzinski. 2004. Electrostatic barrier to recovery of dipalmitoylphosphatidylglycerol monolayers after collapse. *Biophysical Journal* 86(2):897-904.
- Alonso, C., T. Alig, J. Yoon, F. Bringezu, H. Warriner, and J.A. Zasadzinski. 2004. More than a monolayer: Relating lung surfactant structure and mechanics to composition. *Biophysical Journal* 87(6):4188-4202.
- Amirkhanian, J.D., R. Bruni, A.J. Waring, C. Navar, and H.W. Taeusch. 1993. Full-Length Synthetic Surfactant Proteins, Sp-B and Sp-C, Reduce Surfactant Inactivation by Serum. *Biochimica Et Biophysica Acta* 1168(3):315-320.
- Amirkhanian, J.D., R. Bruni, A.J. Waring, and H.W. Taeusch. 1991a. Inhibition of surfactant lipids and synthetic sequences of surfactant proteins SP-B and SP-C. *Biochimica et Biophysica Acta* 1096:355-360.
- Amirkhanian, J.D., R. Bruni, A.J. Waring, and H.W. Taeusch. 1991b. Inhibition of surfactant lipids and synthetic sequences of surfactant proteins SP-B and SP-C. *Biochimica et Biophysica Acta* 1096:355-360.
- Armand, P., K. Kirshenbaum, A. Falicov, R.L. Dunbrack, K.A. Dill, R.N. Zuckermann, and F.E. Cohen. 1997. Chiral N-substituted glycines can form stable helical conformations. *Folding & Design* 2:369-375.
- Armand, P., K. Kirshenbaum, R.A. Goldsmith, S. Farr-Jones, A.E. Barron, K.T.V. Truong, K.A. Dill, D.F. Mierke, F.E. Cohen, R.N. Zuckermann, and E.K. Bradley. 1998. NMR determination of the major solution conformation of a peptoid pentamer with chiral side chains. *Proceedings of the National Academy of Sciences* 95:4309-4314.
- Baatz, J.E., B. Elledge, and J.A. Whitsett. 1990. Surfactant protein SP-B induces ordering at the surface of model membrane bilayers. *Biochemistry* 29:6714-6720.
- Baatz, J.E., V. Sarin, D.R. Absolom, C. Baxter, and J.A. Whitsett. 1991. Effects of Surfactant-Associated Protein Sp-B Synthetic Analogs on the Structure and Surface-Activity of Model Membrane Bilayers. *Chem. Phys. Lipids* 60(2):163-178.
- Beck, D.C., M. Ikegami, C.L. Na, S. Zaltash, J. Johansson, J.A. Whitsett, and T.E. Weaver. 2000. The role of homodimers in surfactant protein B function in vivo. *J. Biol. Chem.* 275(5):3365-3370.
- Bi, X.H., C.R. Flach, J. Perez-Gil, I. Plasencia, D. Andreu, E. Oliveira, and R. Mendelsohn. 2002. Secondary structure and lipid interactions of the N-terminal segment of pulmonary surfactant SP-C in Langmuir films: IR reflection-absorption spectroscopy and surface pressure studies. *Biochemistry* 41(26):8385-8395.
- Borman, S. 1998. Peptoids eyed for gene therapy applications. *Chem. Eng. News* 76(18):56-57.
- Bringezu, F., J. Ding, G. Brezesinski, and J.A. Zasadzinski. 2001. Changes in model lung surfactant monolayers induced by palmitic acid. *Langmuir* 17:4641-4648.
- Bringezu, F., J.Q. Ding, G. Brezesinski, A.J. Waring, and J.A. Zasadzinski. 2002. Influence of pulmonary surfactant protein B on model lung surfactant monolayers. *Langmuir* 18(6):2319-2325.
- Brockman, J.M., Z.D. Wang, R.H. Notter, and R.A. Dluhy. 2003. Effect of hydrophobic surfactant proteins SP-B and SP-C on binary phospholipid monolayers II. Infrared external reflectance-absorption spectroscopy. *Biophysical Journal* 84(1):326-340.

- Bruni, R., H.W. Taeusch, and A.J. Waring. 1991. Surfactant protein B: Lipid interactions of synthetic peptides representing the amino-terminal amphipathic domain. *Proceedings of the National Academy of Sciences* 88(16):7451-7455.
- Clark, J.C., S.E. Wert, C.J. Bachurski, M.T. Stahlman, B.R. Stripp, T.E. Weaver, and J.A. Whitsett. 1995. Targeted Disruption of the Surfactant Protein-B Gene Disrupts Surfactant Homeostasis, Causing Respiratory-Failure in Newborn Mice. *Proceedings of the National Academy of Sciences of the United States of America* 92(17):7794-7798.
- Cochrane, C.G., S.D. Revak, A. Merritt, G.P. Heldt, M. Hallman, M.D. Cunningham, D. Easa, A. Pramanik, D.K. Edwards, and M.S. Alberts. 1996. The efficacy and safety of KL(4)-surfactant in infants with respiratory distress syndrome. *American Journal of Respiratory and Critical Care Medicine* 153(1):404-410.
- Creuwels, L.A.J.M., E.H. Boer, R.A. Demel, L.M.G.v. Golde, and H.P. Haagsman. 1995. Neutralization of the positive charges of surfactant protein C. *J. Biol. Chem.* 270(27):16225-16229.
- Cruz, A., C. Casals, K.M.W. Keough, and J. Perez-Gil. 1997. Different modes of interaction of pulmonary surfactant protein SP-B in phosphatidylcholine bilayers. *Biochemical Journal* 327:133-138.
- Cruz, A., L. Vazquez, M. Velez, and J. Perez-Gil. 2004. Effect of pulmonary surfactant protein SP-B on the micro- and nanostructure of phospholipid films. *Biophysical Journal* 86(1):308-320.
- Davis, A.J., A.H. Jobe, D. Hafner, and M. Ikegami. 1998. Lung function in premature lambs and rabbits treated with a recombinant SP-C surfactant. *American Journal of Respiratory and Critical Care Medicine* 157(2):553-559.
- Dico, A.S., J. Hancock, M.R. Morrow, J. Stewart, S. Harris, and K.M.W. Keough. 1997a. Pulmonary surfactant protein SP-B interacts similarly with dipalmitylphosphatidylglycerol and dipalmitoylphosphatidylcholine in phosphatidylcholine/phosphatidylglycerol mixtures. *Biochemistry* 36:4172-4177.
- Dico, A.S., J. Hancock, M.R. Morrow, J. Stewart, S. Harris, and K.M.W. Keough. 1997b. Pulmonary surfactant protein SP-B interacts similarly with dipalmitylphosphatidylglycerol and dipalmitoylphosphatidylcholine in phosphatidylcholine/phosphatidylglycerol mixtures. *Biochemistry* 36:4172-4177.
- Diemel, R.V., M.M.E. Snel, L.M.G. van Golde, G. Putz, H.P. Haagsman, and J.J. Batenburg. 2002. Effects of cholesterol on surface activity and surface topography of spread surfactant films. *Biochemistry* 41(50):15007-15016.
- Ding, J., D.Y. Takamoto, A.v. Nahmen, M.M. Lipp, K.Y.C. Lee, A.J. Waring, and J.A. Zasadzinski. 2001. Effects of lung surfactant proteins, SP-B and SP-C, and palmitic acid on monolayer stability. *Biophysical Journal* 80:2262-2272.
- Ding, J.Q., I. Doudevski, H.E. Warriner, T. Alig, and J.A. Zasadzinski. 2003. Nanostructure changes in lung surfactant monolayers induced by interactions between palmitoyloleoylphosphatidylglycerol and surfactant protein B. *Langmuir* 19(5):1539-1550.
- Discher, B.M., K.M. Maloney, D.W. Grainger, and S.B. Hall. 2002. Effect of neutral lipids on coexisting phases in monolayers of pulmonary surfactant. *Biophysical Chemistry* 101:333-345.
- Flach, C.R., A. Gericke, K.M.W. Keough, and R. Mendelsohn. 1999. Palmitoylation of lung surfactant protein SP-C alters surface thermodynamics, but not protein secondary

- structure or orientation in 1,2-dipalmitoylphosphatidylcholine Langmuir films. *Biochim. Biophys. Acta-Biomembr.* 1416(1-2):11-20.
- Fleming, B.D., and K.M.W. Keough. 1988. Surface Respreading After Collapse Of Monolayers Containing Major Lipids Of Pulmonary Surfactant. *Chem. Phys. Lipids* 49(1-2):81-86.
- Freites, J.A., Y. Choi, and D.J. Tobias. 2003. Molecular dynamics simulations of a pulmonary surfactant protein B peptide in a lipid monolayer. *Biophysical Journal* 84(4):2169-2180.
- Frerking, I. 2001. Pulmonary surfactant: functions, abnormalities and therapeutic options. *Intensive care medicine* 27(11):1699-1717.
- Gericke, A., C.R. Flach, and R. Mendelsohn. 1997. Structure and orientation of lung surfactant SP-C and L-alpha- dipalmitoylphosphatidylcholine in aqueous monolayers. *Biophysical Journal* 73(1):492-499.
- Gibbons, J.A., A.A. Hancock, C.R. Vitt, S. Knepper, S.A. Buckner, M.E. Brune, I. Milicic, J.F. Kerwin, Jr., L.S. Richter, E.W. Taylor, K.L. Spear, R.N. Zuckermann, D.C. Spellmeyer, R.A. Braeckman, and W.H. Moos. 1996. Pharmacologic characterization of CHIR 2279, an N-substituted glycine peptoid with high-affinity binding for alpha 1-adrenoceptors. *J. Pharmacol. Exp. Ther.* 277(2):885-899.
- Goerke, J. 1997. Pulmonary surfactants - physicochemical aspects. *Curr. Opin. Colloid Interface Sci.* 2(5):526-530.
- Gopal, A., and K.Y.C. Lee. 2001. Morphology and collapse transitions in binary phospholipid monolayers. *J. Phys. Chem. B* 105(42):10348-10354.
- Gordon, L.M., S. Horvath, M.L. Longo, J.A.N. Zasadzinski, H.W. Taeusch, K. Faull, C. Leung, and A.J. Waring. 1996. Conformation and molecular topography of the N-terminal segment of surfactant protein B in structure-promoting environments. *Protein Science* 5:1662-1675.
- Gupta, M., J.M. Hernandez-Juviel, A.J. Waring, and F.J. Walther. 2001. Function and inhibition sensitivity of the N-terminal segment of surfactant protein B (SP-B1-25) in preterm rabbits. *Thorax* 56(11):871-876.
- Gustafsson, M., M. Palmblad, T. Curstedt, J. Johansson, and S. Schürch. 2000. Palmitoylation of a pulmonary surfactant protein C analogue affects the surface associated lipid reservoir and film stability. *Biochim. Biophys. Acta-Biomembr.* 1466(1-2):169-178.
- Gustafsson, M., G. Vandebussche, T. Curstedt, J.M. Ruyschaert, and J. Johansson. 1996. The 21-residue surfactant peptide (LysLeu4)4Lys(KL4) is a transmembrane alpha-helix with a mixed nonpolar/polar surface. *FEBS Letters* 384(2):185-188.
- Hall, S.B., A.R. Venkitaraman, J.A. Whitsett, B.A. Holm, and R.H. Notter. 1992. Importance of hydrophobic apoproteins as constituents of clinical exogenous surfactants. *Annual Review in Respiratory Distress* 145:24-30.
- Haller, T., P. Dietl, H. Stockner, M. Frick, N. Mair, I. Tinhofer, A. Ritsch, G. Enhorning, and G. Putz. 2004. Tracing surfactant transformation from cellular release to insertion into an air-liquid interface. *Am. J. Physiol.-Lung Cell. Mol. Physiol.* 286(5):L1009-L1015.
- Harbottle, R.R., K. Nag, N.S. McIntyre, F. Possmayer, and N.O. Petersen. 2003. Molecular organization revealed by time-of-flight secondary ion mass spectrometry of a clinically used extracted pulmonary surfactant. *Langmuir* 19(9):3698-3704.
- Ingenito, E.P., L.M.J. Morris, F.F. Espinosa, R.D. Kamm, and M. Johnson. 1999. Biophysical characterization and modeling of lung surfactant components. *Journal of Applied Physiology* 86(5):1702-1714.

- Johansson, J. 2003. Molecular determinants for amyloid fibril formation: lessons from lung surfactant protein C. *Swiss Medical Weekly* 133(19-20):275-282.
- Johansson, J., T. Curstedt, and H. Jornvall. 1991. Surfactant protein B: Disulfide bridges, structural properties, and kringle similarities. *Biochemistry* 30:6917-6921.
- Johansson, J., T. Szyperski, T. Curstedt, and K. Wuthrich. 1994. The NMR Structure of the Pulmonary Surfactant-Associated Polypeptide SP-C in an Apolar Solvent Contains a Valyl-Rich Alpha-Helix. *Biochemistry* 33(19):6015-6023.
- Johansson, J., T. Szyperski, and K. Wuthrich. 1995. Pulmonary Surfactant-Associated Polypeptide SP-C in Lipid Micelles - CD Studies of Intact SP-C and NMR Secondary Structure Determination of Depalmitoyl-SP-C(1-17). *FEBS Letters* 362(3):261-265.
- Kirshenbaum, K., A.E. Barron, R.A. Goldsmith, P. Armand, E.K. Bradley, K.T.V. Truong, K.A. Dill, and F.E. Cohen. 1998. Sequence-specific polypeptoids: A diverse family of heteropolymers with stable secondary structure. *Proceedings of the National Academy of Sciences* 95:4303-4308.
- Krol, S., A. Janshoff, M. Ross, and H.-J. Galla. 2000. Structure and function of surfactant protein B and C in lipid monolayers: a scanning force microscopy study. *Physical Chemistry Chemical Physics* 2:4586-4593.
- Larsson, M., K. Larsson, T. Nylander, and P. Wollmer. 2003. The bilayer melting transition in lung surfactant bilayers: the role of cholesterol. *Eur. Biophys. J. Biophys. Lett.* 31(8):633-636.
- Lewis, J.F., Ruud Veldhuizen. 2003. The Role of Exogenous Surfactant in the Treatment of Acute Lung Injury. *Annu. Rev. Physiol.* 65:613-642.
- Lipp, M.M., K.Y.C. Lee, J.A. Zasadzinski, and A.J. Waring. 1996. Phase and morphology changes in lipid monolayers induced by SP- B protein and its amino-terminal peptide. *Science* 273(5279):1196-1199.
- Lipp, M.M., K.Y.C. Lee, J.A. Zasadzinski, and A.J. Waring. 1997. Design and performance of an integrated fluorescence, polarized fluorescence, and Brewster angle microscope Langmuir trough assembly for the study of lung surfactant monolayers. *Rev. Sci. Instrum.* 68(6):2574-2582.
- Longo, M.L., A.M. Bisagno, J.A.N. Zasadzinski, R. Bruni, and A.J. Waring. 1993. A Function of Lung Surfactant Protein Sp-B. *Science* 261(5120):453-456.
- Malcharek, S., A. Hinz, L. Hilterhaus, and H.J. Galla. 2005. Multilayer structures in lipid monolayer films containing surfactant protein C: Effects of cholesterol and POPE. *Biophysical Journal* 88(4):2638-2649.
- Markart, P., C. Ruppert, F. Grimminger, W. Seeger, and A. Gunther. 2003. Fibrinolysis-inhibitory capacity of clot-embedded surfactant is enhanced by SP-B and SP-C. *Am. J. Physiol.-Lung Cell. Mol. Physiol.* 284(1):L69-L76.
- McLean, L.R., and J.E. Lewis. 1995. Biomimetic pulmonary surfactants. *Life Sciences* 56(6):363-378.
- McLean, L.R., J.E. Lewis, K.A. Hagaman, T.J. Owen, and E.R. Matthews. 1993. Role of the Hydrophobic Face of Amphipathic Alpha-Helical Peptides in Synthetic Pulmonary Surfactants. *J. Pharmacol. Exp. Ther.* 266(2):551-556.
- Miller, S.M., R.J. Simon, S. Ng, R.N. Zuckermann, J.M. Kerr, and W.H. Moos. 1995. Comparison of the proteolytic susceptibilities of homologous L-amino acid, D-amino acid, and N-substituted glycine peptide and peptoid oligomers. *Drug Development Research* 35(1):20-32.



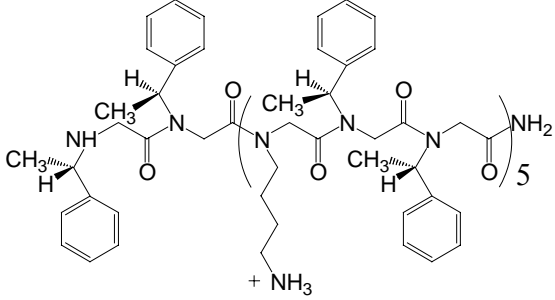
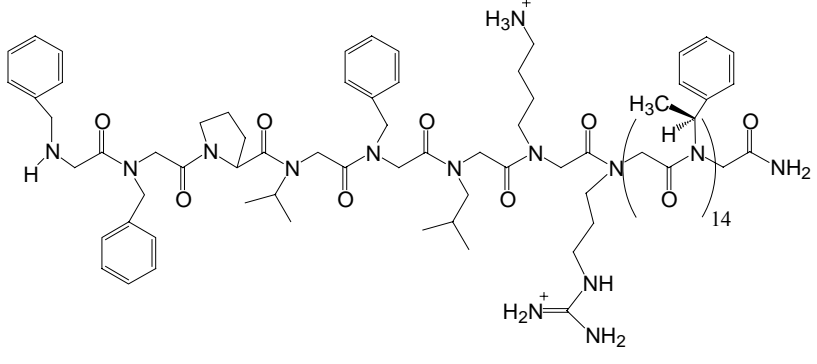
- Morrow, M.R. 2004. Perturbation of DPPC bilayers by high concentrations of pulmonary surfactant protein SP-B. *European Biophysics Journal* 33(4):285-290.
- Nag, K., J. PerezGil, A. Cruz, and K.M.W. Keough. 1996. Fluorescently labeled pulmonary surfactant protein C in spread phospholipid monolayers. *Biophysical Journal* 71(1):246-256.
- Nilsson, G., M. Gustafsson, G. Vandenbussche, E. Veldhuizen, W.J. Griffiths, J. Sjoval, H.P. Haagsman, J.M. Ruysschaert, B. Robertson, T. Curstedt, and J. Johansson. 1998. Synthetic peptide-containing surfactants - Evaluation of transmembrane versus amphipathic helices and surfactant protein C poly-valyl to poly-leucyl substitution. *European Journal of Biochemistry* 255(1):116-124.
- Nogee, L.M. 2004. Alterations in SP-B and SP-C expression in neonatal lung disease. *Annual Review of Physiology* 66:601-623.
- Notter, R.H. 2000a. Clinical Surfactant Replacement Therapy for Neonatal RDS. *In Lung Surfactants: Basic Science and Clinical Applications*. Lenfant C, editor. Marcel Dekker, Inc., New York. 281-298.
- Notter, R.H. 2000b. Diseases of Lung Surfactant Deficiency or Dysfunction. *In Lung Surfactants: Basic Science and Clinical Applications*. Lenfant C, editor. Marcel Dekker, Inc., New York. 233-248.
- Notter, R.H. 2000c. Functional Composition and Component Biophysics of Endogenous Lung Surfactant. *In Lung Surfactants: Basic Science and Clinical Applications*. Lenfant C, editor. Marcel Dekker, Inc., New York. 171-206.
- Notter, R.H. 2000d. Lung Surfactants: Basic Science and Clinical Applications. Lenfant C, editor. Marcel Dekker, New York.
- Notter, R.H. 2000e. Phospholipids: Introduction to Structure and Biophysics. *In Lung Surfactants: Basic Science and Clinical Applications*. Lenfant C, editor. Marcel Dekker, New York. 45-72.
- Notter, R.H., S. Holcomb, and R.D. Mavis. 1980. Dynamic Surface-Properties Of Phosphatidylglycerol-Dipalmitoyl Phosphatidylcholine Mixed Films. *Chem. Phys. Lipids* 27(4):305-319.
- Ogreig, S., and C.B. Daniels. 2001. The roles of cholesterol in pulmonary surfactant: insights from comparative and evolutionary studies. *Comparative Biochemistry and Physiology Part A* 129:75-89.
- Oosterlakendijksterhuis, M.A., H.P. Haagsman, L.M.G. Vangolde, and R.A. Demel. 1991a. Characterization of Lipid Insertion into Monomolecular Layers Mediated by Lung Surfactant Proteins Sp-B and Sp-C. *Biochemistry* 30(45):10965-10971.
- Oosterlakendijksterhuis, M.A., H.P. Haagsman, L.M.G. Vangolde, and R.A. Demel. 1991b. Interaction of Lipid Vesicles with Monomolecular Layers Containing Lung Surfactant Proteins Sp-B or Sp-C. *Biochemistry* 30(33):8276-8281.
- Oosterlakendijksterhuis, M.A., M. Vaneijk, L.M.G. Vangolde, and H.P. Haagsman. 1992. Lipid Mixing Is Mediated by the Hydrophobic Surfactant Protein Sp-B but Not by Sp-C. *Biochimica Et Biophysica Acta* 1110(1):45-50.
- Palmblad, M., J. Johansson, B. Robertson, and T. Curstedt. 1999. Biophysical activity of an artificial surfactant containing an analogue of surfactant protein (SP)-C and native SP-B. *Biochemical Journal* 339:381-386.

- Plasencia, I., A. Cruz, C. Casals, and J. Perez-Gil. 2001. Superficial disposition of the N-terminal region of the surfactant protein SP-C and the absence of specific SP-B-SP-C interactions in phospholipid bilayers. *Biochemical Journal* 359:651-659.
- Plasencia, I., L. Rivas, K.M.W. Keough, D. Marsh, and J. Perez-Gil. 2004. The N-terminal segment of pulmonary surfactant lipopeptide SP-C has intrinsic propensity to interact with and perturb phospholipid bilayers. *Biochemical Journal* 377:183-193.
- Poynter, S.E., and A.M. LeVine. 2003. Surfactant biology and clinical application. *Critical Care Clinics* 19(3):459-472.
- Putz, G., J. Goerke, H.W. Tausch, and J.A. Clements. 1994. Comparison of captive and pulsating bubble surfactometers with use of lung surfactants. *Journal of Applied Physiology* 76(4):1425-1431.
- Qanbar, R., S. Cheng, F. Possmayer, and S. Schurch. 1996. Role of the palmitoylation of surfactant-associated protein C in surfactant film formation and stability. *Am. J. Physiol.-Lung Cell. Mol. Physiol.* 15(4):L572-L580.
- Robillard, E. 1964. Microaerosol administration of synthetic beta-gamma-dipalmitoyl-l-alpha-lecithin in respiratory distress syndrome - preliminary report. *CMAJ* 90(2):55.
- Sanborn, T.J., C.W. Wu, R.N. Zuckerman, and A.E. Barron. 2002. Extreme stability of helices formed by water-soluble poly-N- substituted glycines (polypeptoids) with alpha-chiral side chains. *Biopolymers* 63(1):12-20.
- Scarpelli, E.M., E. David, M. Cordova, and A.J. Mautone. 1992. Surface-Tension of Therapeutic Surfactants (Exosurf Neonatal, Infasurf, and Survanta) as Evaluated by Standard Methods and Criteria. *Am. J. Perinatol.* 9(5-6):414-419.
- Schram, V., and S.B. Hall. 2004. SP-B and SP-C Alter Diffusion in Bilayers of Pulmonary Surfactant. *Biophys. J.* 86(6):3734-3743.
- Seurnyck, S.L., N.J. Brown, C.W. Wu, K.W. Germino, E.K. Kohlmeir, E.P. Ingenito, M.R. Glucksberg, A.E. Barron, and M. Johnson. 2005a. Optical monitoring of bubble size and shape in a pulsating bubble surfactometer. *Journal Of Applied Physiology* 99(2):624-633.
- Seurnyck, S.L., J.A. Patch, and A.E. Barron. 2005b. Simple, helical peptoid analogs of lung surfactant protein B. *Chem. Biol.* 12(1):77-88.
- Simon, R.J., R.S. Kania, R.N. Zuckermann, V.D. Huebner, D.A. Jewell, S. Banville, S. Ng, L. Wang, S. Rosenberg, and et al. 1992. Peptoids: a modular approach to drug discovery. *Proc. Natl. Acad. Sci. U. S. A.* 89(20):9367-9371.
- Suresh, G.K., and R.F. Soll. 2003. Exogenous surfactant therapy in newborn infants. *Annals Academy of Medicine Singapore* 32(3):335-345.
- Takamoto, D.Y., M.M. Lipp, A.v. Nahmen, K.Y.C. Lee, A.J. Waring, and J.A. Zasadzinski. 2001. Interaction of lung surfactant proteins with anionic phospholipids. *Biophysical Journal* 81:153-169.
- Takei, T., Y. Hashimoto, T. Aiba, K. Sakai, and T. Fujiwara. 1996a. The surface properties of chemically synthesized peptides analogous to human pulmonary surfactant protein SP-C. *Biological and Pharmaceutical Bulletin* 19(10):1247-1253.
- Takei, T., Y. Hashimoto, E. Ohtsubo, K. Sakai, and H. Ohkawa. 1996b. Characterization of poly-leucine substituted analogues of the human surfactant protein SP-C. *Biol. Pharmacol. Bull.* 19(12):1550-1555.
- Tanaka, Y., T. Takei, T. Aiba, K. Masuda, A. Kiuchi, and T. Fujiwara. 1986. Development of synthetic lung surfactants. *Journal of Lipid Research* 27:475-485.

- Taneva, S., and K. Keough. 1994a. Pulmonary surfactant proteins SP-B and SP-C in spread monolayers at the air-water interface: III. Proteins SP-B plus SP-C with phospholipids in spread monolayers. *Biophys. J.* 66(4):1158-1157.
- Taneva, S., and K.M.W. Keough. 1997. Cholesterol modifies the properties of surface films of dipalmitoylphosphatidylcholine plus pulmonary surfactant-associated protein B or C spread or adsorbed at the air-water interface. *Biochemistry* 36(4):912-922.
- Taneva, S.G., and K.M.W. Keough. 1994b. Dynamic surface properties of pulmonary surfactant proteins SP-B and SP-C and their mixtures with dipalmitoylphosphatidylcholine. *Biochemistry* 33:14660-14670.
- Tolle, A., W. Meier, M. Rudiger, K.P. Hofmann, and B. Rustow. 2002. Effect of cholesterol and surfactant protein B on the viscosity of phospholipid mixtures. *Chem. Phys. Lipids* 114(2):159-168.
- Vandenbussche, G., A. Clercx, M. Clercx, T. Cirstedt, J. Johansson, H. Jornvall, and J.-M. Ruyschaert. 1992. Secondary structure and orientation of the surfactant protein SP-B in a lipid environment. A Fourier Transform Infrared Spectroscopy study. *Biochemistry* 31:9169-9176.
- Veldhuizen, E.J.A., J.J. Batenburg, L.M.G.v. Golde, and H.P. Haagsman. 2000. The role of surfactant proteins in DPPC enrichment of surface films. *Biophysical Journal* 79:3164-3171.
- Veldhuizen, R., K. Nag, S. Orgeig, and F. Possmayer. 1998. The role of lipids in pulmonary surfactant. *Biochimica et Biophysica Acta* 1408:90-108.
- Vorbroker, D.K., S.A. Profitt, L.M. Noguee, and J.A. Whitsett. 1995. Aberrant Processing of Surfactant Protein-C in Hereditary Sp-B Deficiency. *Am. J. Physiol.-Lung Cell. Mol. Physiol.* 12(4):L647-L656.
- Walther, F.J., L.M. Gordon, J.A. Zasadzinski, M.A. Sherman, and A.J. Waring. 2000. Surfactant protein B and C analogues. *Mol. Genet. Metab.* 71:342-351.
- Walther, F.J., J.M. Hernandez-Juviel, L.M. Gordon, A.J. Waring, P. Stenger, and J.A. Zasadzinski. 2005. Comparison of three lipid formulations for synthetic surfactant with a surfactant protein B analog. *Exp. Lung Res.* 31(6):563-579.
- Walther, F.J., J.M. Hernandez-Juviel, P.E. Mercado, L.M. Gordon, and A.J. Waring. 2002. Surfactant with SP-B and SP-C analogues improves lung function in surfactant-deficient rats. *Biology of the Neonate* 82(3):181-187.
- Wang, Z., S.B. Hall, and R.H. Notter. 1996. Roles of different hydrophobic constituents in the adsorption of pulmonary surfactant. *J. Lipid Res.* 37:790-798.
- Waring, A., H.W. Taeusch, R. Bruni, J. Amirkhanian, B.C.R. Fan, R. Stevens, and J. Young. 1989. Synthetic amphipathic sequences of surfactant protein B mimic several physiochemical and in vivo properties of native pulmonary surfactant proteins. *Peptide Research* 2(5):308-313.
- Wu, C.W., T.J. Sanborn, K. Huang, R.N. Zuckermann, and A. Barron. 2001. Peptoid oligomers with  $\alpha$ -chiral, aromatic side chains: Sequence requirements for the formation of stable peptoid helices. *J. Am. Chem. Soc.* 123:6778-6784.
- Wu, C.W., S.L. Seurnyck, K.Y.C. Lee, and A.E. Barron. 2003. Helical peptoid mimics of lung surfactant protein C. *Chemistry & Biology* 10(11):1057-1063.
- Wustneck, N., R. Wustneck, V.B. Fainerman, R. Miller, and U. Pison. 2001. Interfacial behavior and mechanical properties of spread lung surfactant protein/lipid layers. *Colloids and Surfaces B: Biointerfaces* 21:191-205.

- Wustneck, N., R. Wustneck, J. Perez-Gil, and U. Pison. 2003. Effects of oligomerization and secondary structure on the surface behavior of pulmonary surfactant proteins SP-B and SP-C. *Biophysical Journal* 84(3):1940-1949.
- Yu, S.-H., and F. Possmayer. 1993. Adsorption, compression and stability of surface films from natural, lipid extract and reconstituted pulmonary surfactants. *Biochimica et Biophysica* 1167:264-271.
- Yu, S.H., and F. Possmayer. 1990. Role of Bovine Pulmonary Surfactant-Associated Proteins in the Surface-Active Property of Phospholipid Mixtures. *Biochimica Et Biophysica Acta* 1046(3):233-241.
- Zuckermann, R.N., J.M. Kerr, S.B.H. Kent, and W.H. Moos. 1992. Efficient method for the preparation of peptoids [oligo(N-substituted glycines)] by submonomer solid-phase synthesis. *J. Am. Chem. Soc.* 114(26):10646-10647.

**Table 1:** Peptide and peptoid sequences and molecular weights.

Molecule	Sequence/Structure	Molecular Weight (Da)
SP-B <sub>1-25</sub>	FPIPLPYAWLARALIKRIQAMIPKG	2866
Peptoid B	 <p>The structure shows a peptoid backbone with a central 1,4-diazepane ring. It features three side chains: a benzyl group, a 1-phenylethyl group, and a 1-phenylethyl group. The backbone ends with a primary amide group (NH<sub>2</sub>) and a quaternary ammonium group (+NH<sub>3</sub>).</p>	2592
SP-C <sub>F,F</sub>	FGIPFFPVHLKRLILLILLILLILLILGALLMGL	3924
Peptoid C	 <p>The structure shows a complex peptoid backbone with multiple side chains including benzyl, isopropyl, and a quaternary ammonium group. It also features a guanidinium group and a primary amide group (NH<sub>2</sub>).</p>	3309

**Table 2:** Mole percentages of added peptide or peptoid in each lipid formulation.

	<b>PCPG (mole%)</b>	<b>TL (mole%)</b>	<b>IL (mole%)</b>
SP-B <sub>1-25</sub> /Peptoid B	2.53	2.16	2.44
SP-C <sub>F,F</sub> /Peptoid C	1.86	1.59	1.78

## Figure Legends

**Figure 1:** Surface pressure-surface area isotherms obtained using the Langmuir-Wilhelmy surface balance at 25 °C (A) and 37 °C (B) for PCPG lipids (solid line), Tanaka lipids (dotted line), and synthetic Infasurf lipids (dashed line).

**Figure 2:** Fluorescent microscopic images of PCPG lipids (A, B), Tanaka lipids (C, D), and synthetic Infasurf lipids (E, F) at  $\sim 35$  mN/m (A, C, E) and  $\sim 50$  mN/m (B, D, F) on buffer at 37 °C, collected with a barrier speed of 5 mm/min.

**Figure 3:** Static bubble (A) and dynamic bubble (B) adsorption results from the pulsating bubble surfactometer in buffer at 37 °C for PCPG lipids (solid line), Tanaka lipids (dotted line), and synthetic Infasurf lipids (dashed line). Dynamic data were collected at 20 cycles/min and loop directions are clockwise.

**Figure 4:** Surface pressure-surface area isotherms obtained using the Langmuir-Wilhelmy surface balance at 37 °C for PCPG lipids (A-B), Tanaka lipids (C-D), and synthetic Infasurf lipids (E-F) with added SP-B (A, C, E) or SP-C mimics (B, D, F). Lipids alone – solid line; lipids + SP-B<sub>1-25</sub> – dotted line; lipids + Peptoid B – xxx; lipids + SP-C<sub>F,F</sub> – dashed line; and lipids + Peptoid C – +++.

**Figure 5:** Fluorescent microscopic images for PCPG lipids (A and B), PCPG lipids with added SP-B<sub>1-25</sub> (C and D), Peptoid B (E and F), SP-C<sub>F,F</sub> (G and H), and Peptoid C (I and J) on buffer at 37 °C, collected with a barrier speed of 5 mm/min. Images shown for  $\Pi \sim 35$  mN/m (A, C, E, G, and I) and  $\Pi \sim 50$  mN/m (B, D, F, H, and J).

**Figure 6:** Fluorescent microscopic images for Tanaka lipids (A and B), Tanaka lipids with added SP-B<sub>1-25</sub> (C and D), Peptoid B (E and F), SP-C<sub>F,F</sub> (G and H), and Peptoid C (I and J) on

buffer at 37 °C, collected with a barrier speed of 5 mm/min. Images shown for  $\Pi \sim 35$  mN/m (A, C, E, G, and I) and  $\Pi \sim 50$  mN/m (B, D, F, H, and J).

**Figure 7:** Fluorescent microscopic images for synthetic Infasurf lipids (A and B), synthetic Infasurf lipids with added SP-B<sub>1-25</sub> (C and D), Peptoid B (E and F), SP-C<sub>F,F</sub> (G and H), and Peptoid C (I and J) on buffer at 37 °C, collected with a barrier speed of 5 mm/min. Images shown for  $\Pi \sim 35$  mN/m (A, C, E, G, and I) and  $\Pi \sim 50$  mN/m (B, D, F, H, and J).

**Figure 8:** Static bubble adsorption results from the pulsating bubble surfactometer in buffer at 37 °C for PCPG lipids (A-B), Tanaka lipids (C-D), and synthetic Infasurf lipids (E-F) with added SP-B (A, C, E) or SP-C mimics (B, D, F). Lipids alone – solid line; lipids + SP-B<sub>1-25</sub> – dotted line; lipids + Peptoid B – xxx; lipids + SP-C<sub>F,F</sub> – dashed line; and lipids + Peptoid C – +++.

**Figure 9:** Dynamic bubble adsorption results from the pulsating bubble surfactometer in buffer at 37 °C for PCPG lipids (A-B), Tanaka lipids (C-D), and synthetic Infasurf lipids (E-F) with added SP-B (A, C, E) or SP-C mimics (B, D, F). Lipids alone – solid line; lipids + SP-B<sub>1-25</sub> – dotted line; lipids + Peptoid B – xxx; lipids + SP-C<sub>F,F</sub> – dashed line; and lipids + Peptoid C – +++.

Data were collected at 20 cycles/min and loop directions are clockwise.



**Figure 1**

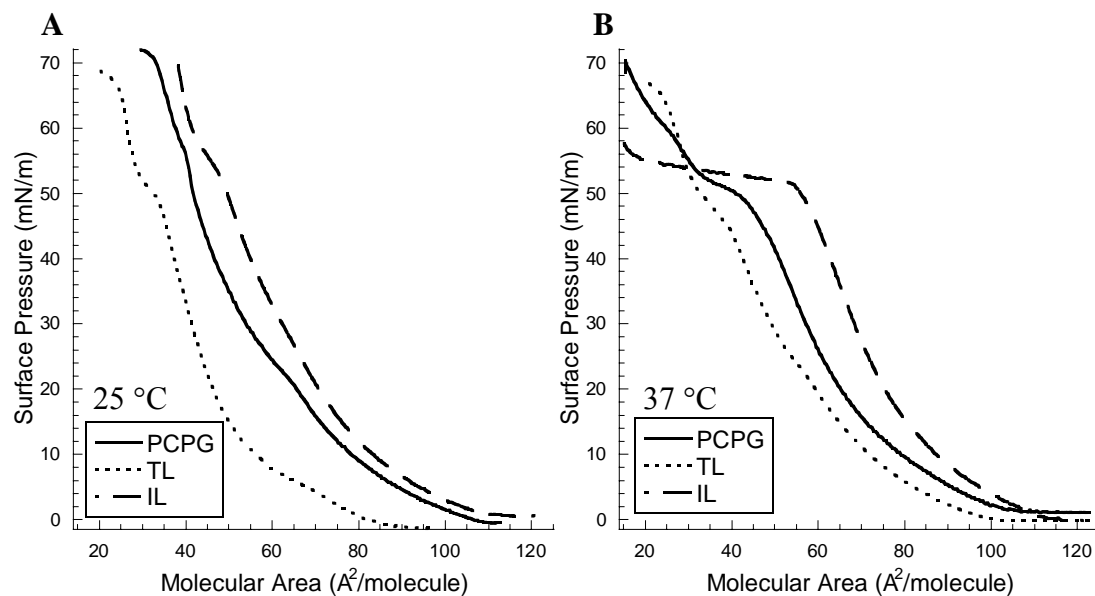


**Figure 2**

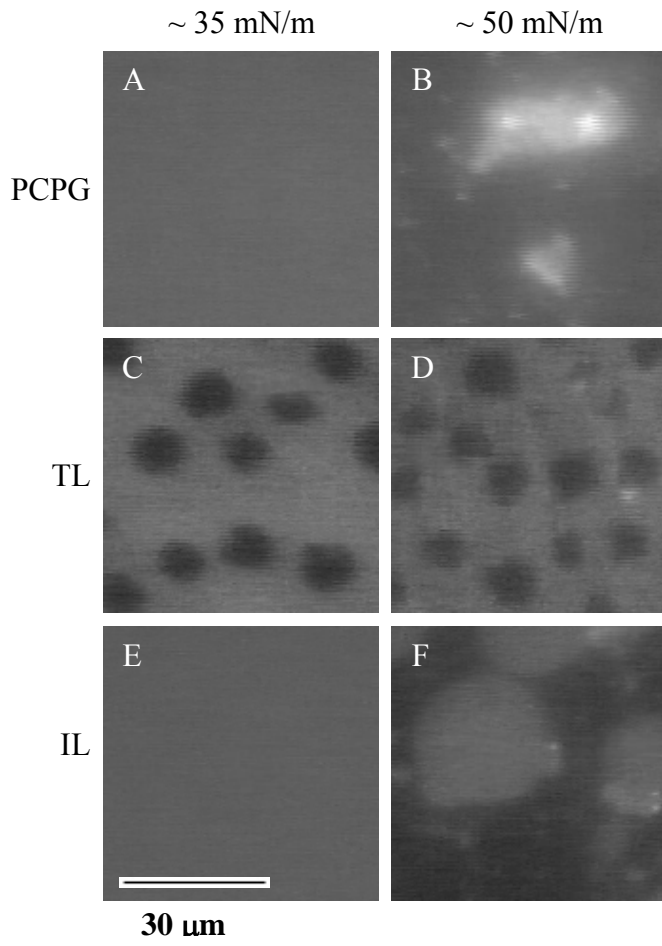


**Figure 3**

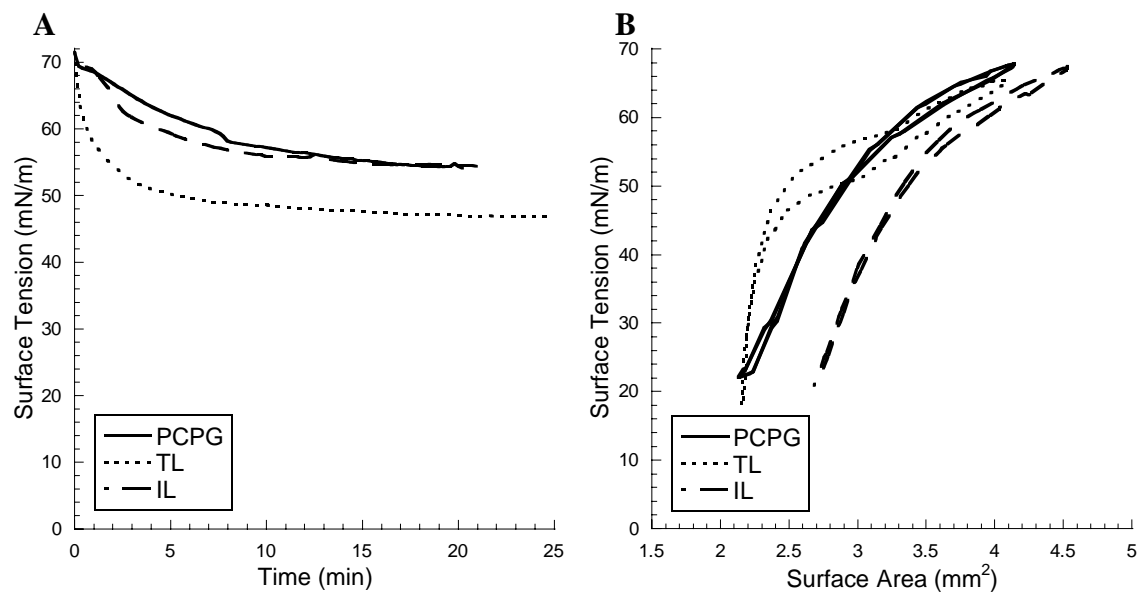


**Figure 4**

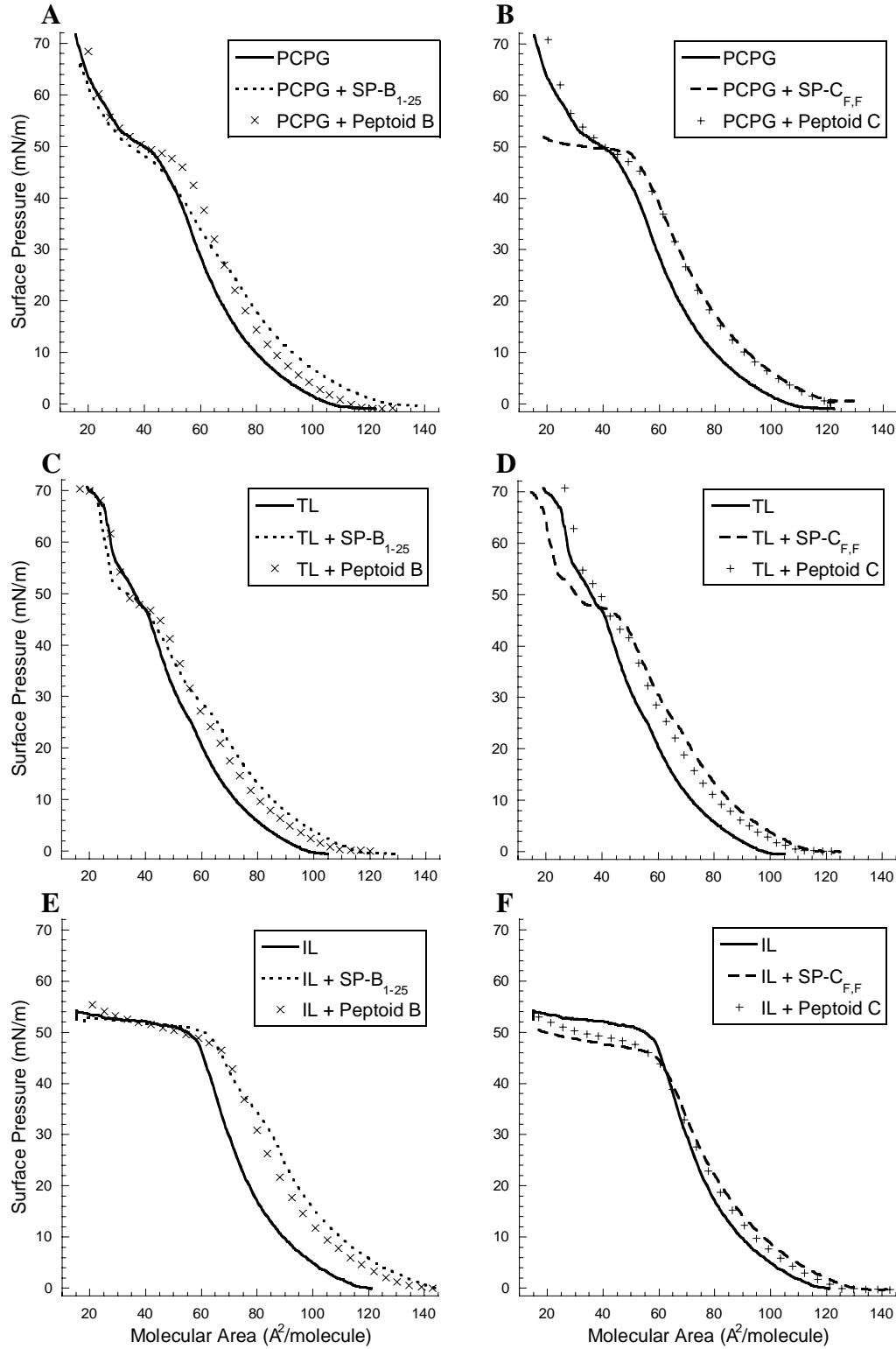


**Figure 5**

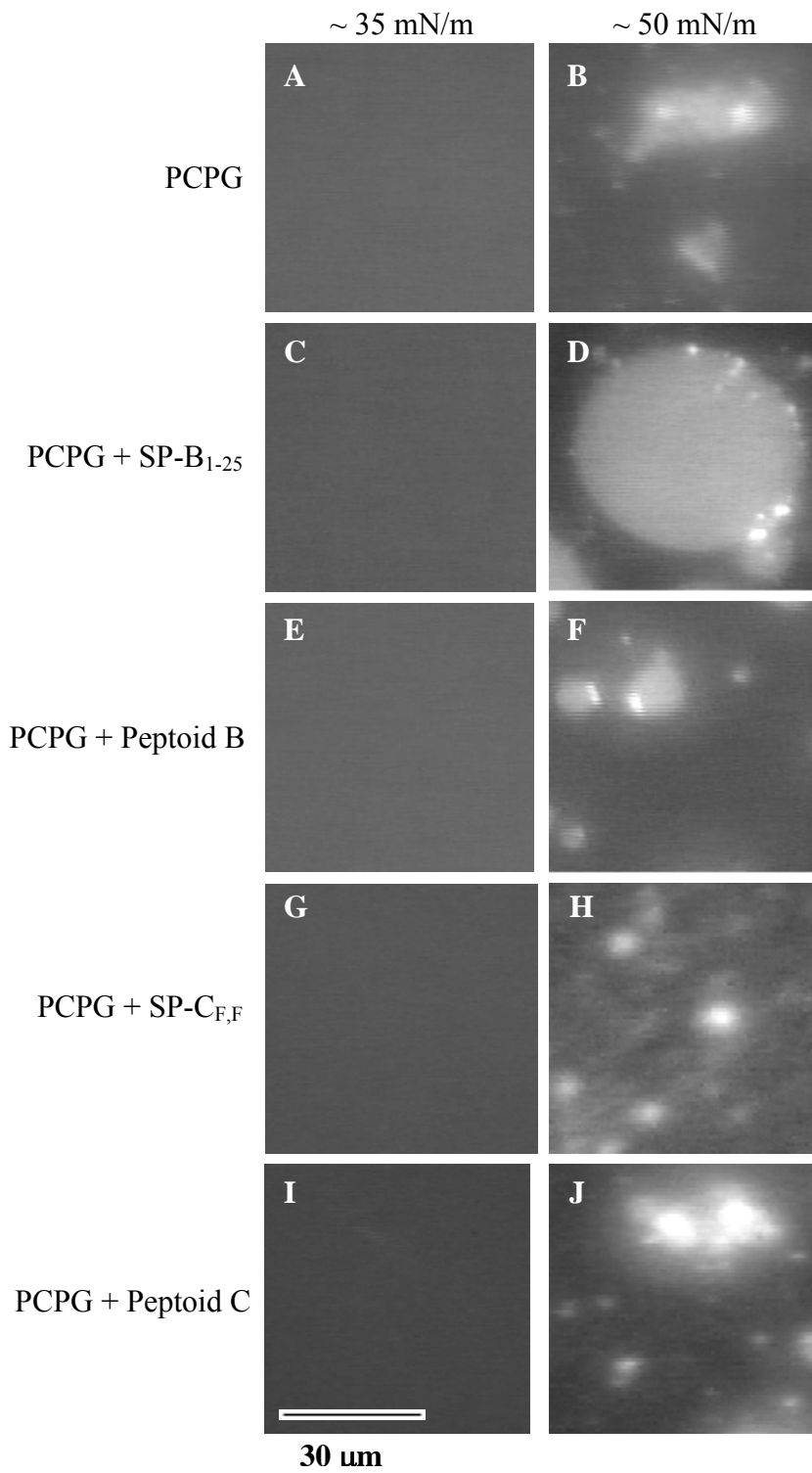


**Figure 6**

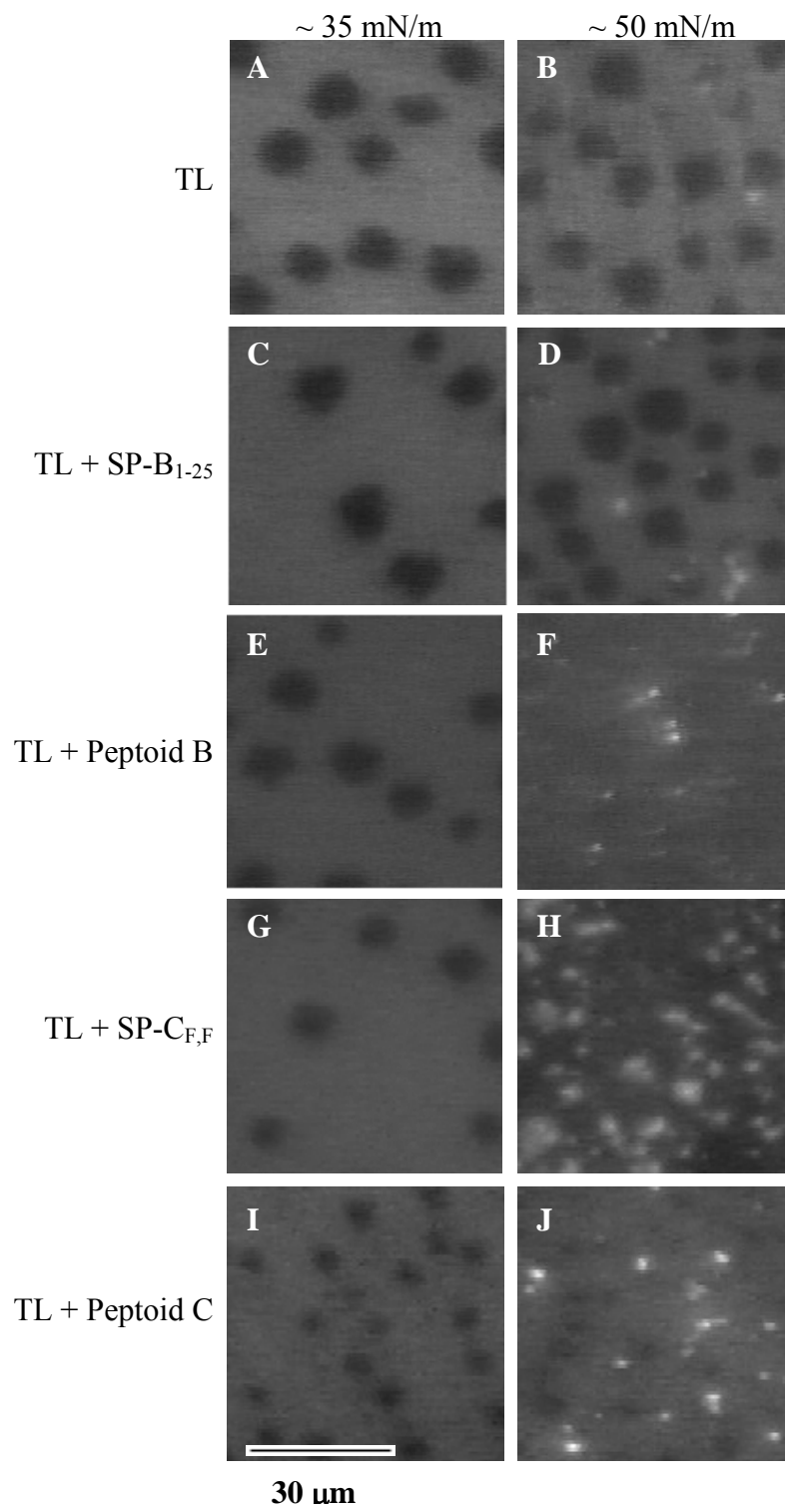


**Figure 7**

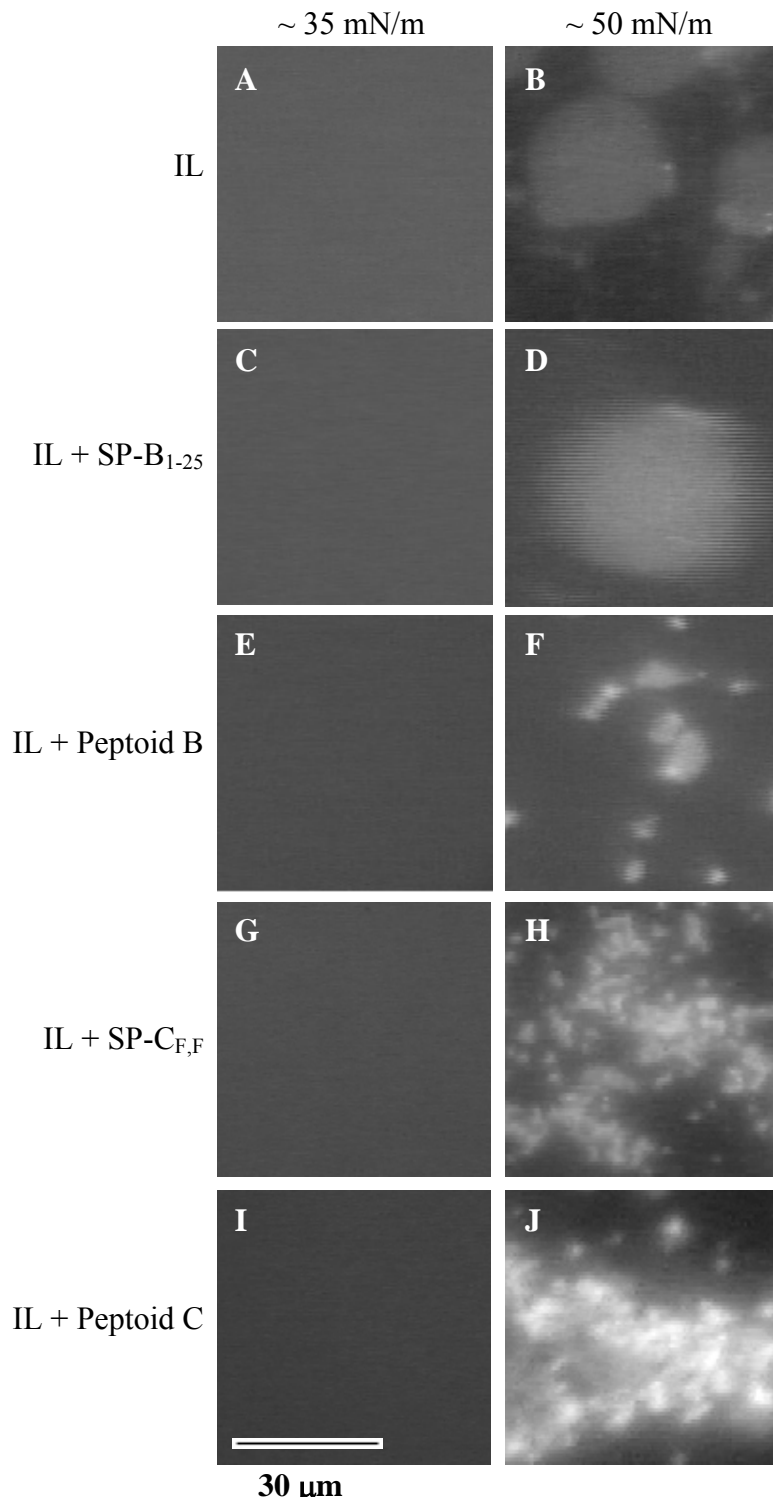


**Figure 8**

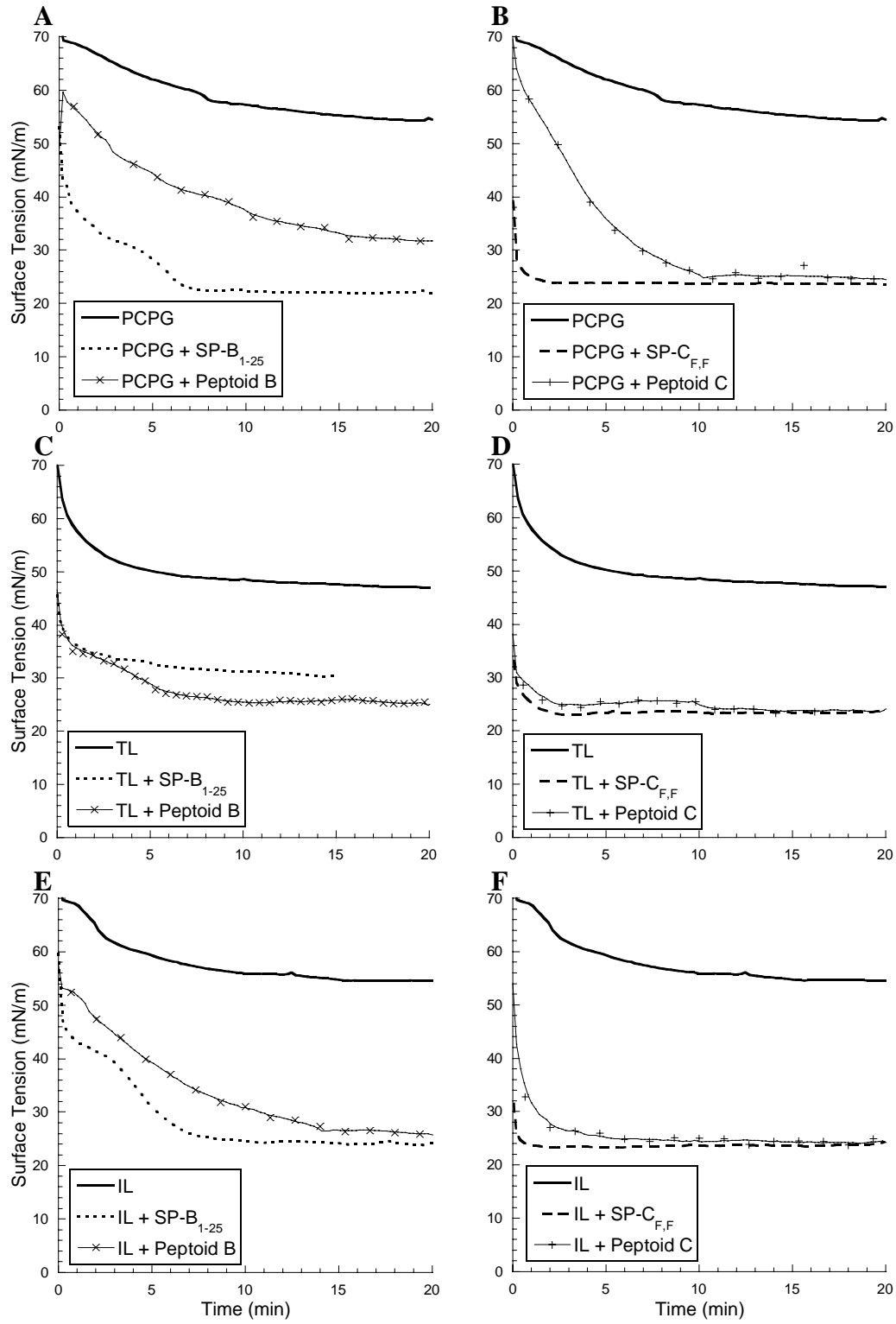




**Figure 9**

